Article

Applications of the Google Earth Engine and Phenology-Based Threshold Classification Method for Mapping Forest Cover and Carbon Stock Changes in Siem Reap Province, Cambodia

Manjunatha Venkatappa [1,2,3,*] [iD], **Nophea Sasaki** [4] [iD], **Sutee Anantsuksomsri** [1,2] [iD] and **Benjamin Smith** [5,6]

1   Regional Urban and Built Environmental Analytics, Faculty of Architecture, Chulalongkorn University, 254 Phayathai Road, Pathumwan, Bangkok 10330, Thailand; sutee.a@chula.ac.th
2   Department of Urban and Regional Planning, Faculty of Architecture, Chulalongkorn University, 254 Phayathai Road, Pathumwan, Bangkok 10330, Thailand
3   LEET intelligence Co., Ltd., Perfect Park, Suan Prikthai, Muang Pathum Thani, Pathum Thani 12000, Thailand
4   Natural Resources Management, School of Environment, Resources and Development, Asian Institute of Technology. P.O. Box 4, Khlong Luang, Pathumthani 12120, Thailand; nopheas@ait.ac.th
5   Hawkesbury Institute for the Environment, Western Sydney University, Bourke St, Richmond, Sydney, NSW 2753, Australia; ben.smith@westernsydney.edu.au
6   Department of Physical Geography and Ecosystem Science, Sölvegatan 12, Lund University, S-223 62 Lund, Sweden
*   Correspondence: Venkatappa.M@chula.ac.th

check for updates

Abstract: Digital and scalable technologies are increasingly important for rapid and large-scale assessment and monitoring of land cover change. Until recently, little research has existed on how these technologies can be specifically applied to the monitoring of Reducing Emissions from Deforestation and Forest Degradation (REDD+) activities. Using the Google Earth Engine (GEE) cloud computing platform, we applied the recently developed phenology-based threshold classification method (PBTC) for detecting and mapping forest cover and carbon stock changes in Siem Reap province, Cambodia, between 1990 and 2018. The obtained PBTC maps were validated using Google Earth high resolution historical imagery and reference land cover maps by creating 3771 systematic 5 × 5 km spatial accuracy points. The overall cumulative accuracy of this study was 92.1% and its cumulative Kappa was 0.9, which are sufficiently high to apply the PBTC method to detect forest land cover change. Accordingly, we estimated the carbon stock changes over a 28-year period in accordance with the Good Practice Guidelines of the Intergovernmental Panel on Climate Change. We found that 322,694 ha of forest cover was lost in Siem Reap, representing an annual deforestation rate of 1.3% between 1990 and 2018. This loss of forest cover was responsible for carbon emissions of 143,729,440 $MgCO_2$ over the same period. If REDD+ activities are implemented during the implementation period of the Paris Climate Agreement between 2020 and 2030, about 8,256,746 $MgCO_2$ of carbon emissions could be reduced, equivalent to about USD 6-115 million annually depending on chosen carbon prices. Our case study demonstrates that the GEE and PBTC method can be used to detect and monitor forest cover change and carbon stock changes in the tropics with high accuracy.

Keywords: Landsat-8; Landsat TM; Google Earth Engine; tropical forestry; forest carbon stocks; emission reductions; REDD+; PBTC

1. Introduction

The rapid loss of forest cover and acceleration of forest degradation in the tropics have been caused by land clearing, burning, and overexploitation [1,2]. A recent study using remote sensing technology revealed that tropical forests have been degraded drastically since 2000 [3]. Selective logging was a main driver of forest degradation, causing the degradation of approximately 400 million ha of tropical forests [4,5]. In addition to rapid forest degradation, deforestation remains high in the tropics. A recent report by the Food and Agriculture Organization of the United Nations (FAO) stated that global forests were reduced by 178 million ha from 1990 to 2000 [6]. More specifically, annual losses of tropical forests were 7.8 million ha in 1990–2000, 5.2 million ha in 2000–2010, and 4.7 million ha in 2010–2020 [6]. Such losses and forest degradation account for about 20% of total global emissions, and represent the second largest source of global emissions [7].

To reduce these losses, several major international agreements have been reached. Reducing Emissions from Deforestation and Forest Degradation (REDD+) of the United Nations Framework Convention on Climate Change (UNFCCC) is one of these agreements and is a result-based financial scheme for reducing carbon emissions or increasing removals in the tropics in exchange for financial compensation. This compensation can occur only if the REDD+ activities are monitored, measured, and verified, and the actual emissions are below the Forest Reference Emission Level (FREL) [8,9]. Therefore, methods for monitoring, reporting, and verifying (MRV) carbon emissions, reductions, or removals are critically needed so that the results from the implementation of the REDD+ activities can be reported on a regular basis. Forest inventories are the commonly used input for MRV purposes. One of these purposes is the establishment of the FREL because it is a benchmark emission against which emission reductions or removals (results) can be assessed for financial incentives [10,11]. Other field-based measurement approaches use the real weight of all parts of all trees in the targeted sample plots to determine forest biomasses using allometric equations (e.g., diameter at breast height and tree height obtained from field-based forest inventory methods) to convert inventory measurements into biomass estimates [12,13]. Although these methods provide the most accurate assessment of biomasses and carbon stocks, they are time consuming [12,14–16], costly and difficult to scale [17,18].

Satellite remote sensing technologies provide an alternative approach to MRV tasks required for the REDD+ scheme in developing countries in the tropics, where the availability of field measurements is sparse [19]. In recent years, phenology-based classification methods using spectral remote sensing data and the enhanced vegetation index (EVI) have shown satisfactory accuracy [20–24]. Previous research [24,25] has shown promising results with high reliability and accuracy for vegetation [26], cropland [27] and land cover mapping [24,28]. The most recent studies classified land cover categories and changes using the moderate to high spatial resolution of the Landsat remote sensing data [24,29,30]. Based on moderate-solution satellite remote sensing data, other studies used basic image analysis techniques such as the maximum likelihood, artificial neural network, decision tree, support vector machine and random forest techniques to classify land cover categories [31,32] using various commercial image processing tools [33,34]. However, these methods are not without challenges such as the costs of acquiring remote sensing time series data, limitation of the spatial extent, variation of spectral properties, acquisition conditions, atmospheric perturbations, data storage, and the limit of image processing speed [35,36]. Many of these challenges can be overcome using features inherent available in the Google Earth Engine (GEE) and its phenology-based threshold classification (PBTC) methods [24]. GEE's cloud computing capability has the potential to quantify vegetation and land cover change, and assess ecosystem dynamics, in a short time at no cost [37]. Furthermore, a larger quantity of training data may not be required for image classification when the GEE PBTC method is used.

The use of PBTC methods in the remote sensing field (including GEE) has raised public and scientific attention because these methods have shown promising results with high accuracy for land cover mapping using moderate to high spatial resolution satellite data [26,38]. Previous research has attempted to study the surface vegetation phenology such as the phenology of natural vegetation, rubber plantations, and rice for land cover mapping in tropical regions [21,23,39,40]. For example,

Venkatappa et al. [24] determined threshold values for 12 land cover categories by assessing the phenological characteristics of each land cover category during the mid-dry phenological season. They used GEE's harmonic model function for Landsat 5 Thematic Mapper (TM) and Landsat Operational Land Imager (OLI) EVI time series data to develop a PBTC method by applying the appropriate algorithms for classifying Landsat imagery [24]. Although a combination of GEE and phenology-based approaches can be used to estimate forest carbon stocks, emissions and removals from deforestation and forest degradation activities in the tropics, only a handful of studies exist on the applications of these approaches despite their importance for performing the MRV tasks of the REDD+ scheme [41].

This study aims to apply the PBTC method for detecting and mapping the forest cover and carbon stock changes by different land cover categories using the available Landsat 5 and Landsat 8 satellite remote sensing data in GEE over the last 28 years from 1990 to 2018. We chose Siem Reap province, Cambodia, as our case study location because of its strategic location, in which all major forest types in Cambodia are found. This study was designed to provide a review of the PBTC method and the required data and description of various steps and methods for establishing the subnational FREL and project emission level. Subsequently, carbon emission reductions and potential carbon revenues were estimated. These are discussed and policy recommendations are presented to achieve the result-based payments from the REDD+ scheme.

2. Materials and Methods

2.1. Study Area

Siem Reap province has 12 districts as shown in Figure 1. It ranks as one of the 10 largest provinces in Cambodia. Siem Reap is located in a tropical area from 14.8 °N to 9.9 °N, and from 102.2 °E to 107.9 °E. The elevation ranges from 6 m above sea level at Tonle Sap lake (the largest freshwater lake in Southeast Asia) to 469 m on Phnom Kulen mountain National Park. The landscape is a mosaic of dryland and edaphic forests, rice fields, shifting cultivation, and urban areas (Figure 1). Landscape patterns and particularly vegetation phenology are influenced by inter and intra annual precipitation patterns [42] as seasonal monsoons bring wet, moisture-rich air from the southwest from May to November, whereas December to April is characterized by drier, cooler air that flows from the northeast. Most of the rainfall occurs during the wet season with an annual precipitation range from 1050 to 1800 mm [43]. The total population in the Siem Reap province increased from 896,443 in 2008 to 1,006,512 in 2019, with an annual growth rate of 1.1% [44]. Siem Reap receives a large number of tourists each year because it hosts the World Heritage Site, Angkor Archeologic Park. It hosted 2.2 million tourists in 2018, increasing from 2.1 million in 2015 [45].
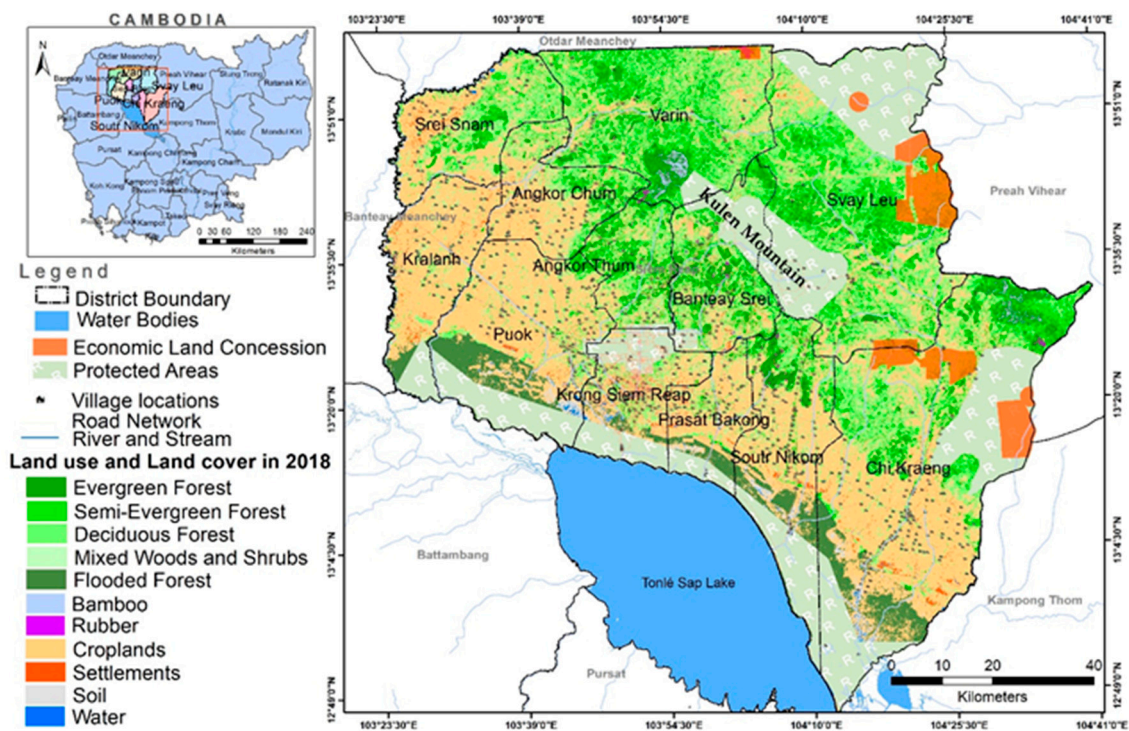
Figure 1. Major land use and land cover categories in Siem Reap province, 2018. Note: The base map data—including district boundary, water bodies, economic land concession boundaries, protected areas, village locations, road and stream network vector data—were collected from open development Cambodia [46]. The land cover map of 2018 was produced from this study.

Siem Reap was chosen for this study because it has all land cover categories except mangrove forest. The major forest types are Evergreen, Semi-Evergreen, Deciduous, Mixed Woods and Shrubs, Bamboo, and Flooded forest [24]. The provincial economy is dominated by agriculture and tourism [47]. Forest resources are important to the local poor because of their high dependency on forest ecosystem services for their livelihoods [47]. The majority of the rural residents depend on the forest products for a living [48].

2.2. Google Earth Engine Remote Sensing Data

The Google Earth Engine offers georeferenced and atmospherically corrected real-time remote sensing data with calibrated top-of-atmosphere reference (TOA) imagery of the entire Landsat satellite image collections, comprising more than 40 years of data. These collections are free of charge for education and natural and environmental research applications [37,49]. In this study, we collected Landsat 5 TOA data from 1990 to 2010 and Landsat 8 OLI TOA data from 2015 to 2018 covering the entire Siem Reap province. Table 1 illustrates the open-access Landsat datasets in GEE from 1990 to 2018 at five-year intervals.

Table 1. Google Earth Engine Landsat collections for the phenology-based threshold classification method (PBTC) and the assessment of carbon stock changes in Siem Reap province over 28 years.

Cloud-Free Month and Year	Path/Raw	Landsat (30 m)	Selected Bands for Median Enhanced Vegetation Index	Number of Image Collections
December–March 1989–1990	126/50 127/51	TM-TOA	4,3,1	11
December–March 1994–1995	126/51 127/50	TM-TOA	4,3,1	21
December–March 1999–2000	126/51 167/50	TM-TOA	4,3,1	19
December–March 2004–2005	126 /51 127/50	TM-TOA	4,3,1	19
December–March 2009–2010	126/51 127/50	TM-TOA	4,3,1	14
December–March 2014–2015	126/51 127/50	OLI-TOA	5,4,2	20
December–March 2017–2018	126/51 127/50	OLI-TOA	5,4,2	20
Total				124

Note: TM, Landsat Thematic Mapper 5; TOA, top-of-atmosphere reflectance; OLI, Landsat Operational Land Imager 8; EVI, enhanced vegetation index. Based on our previous study [24], we selected the image collections during the end of the season (December to March) and composited 4 months of imagery, including one month of the previous year (December), to obtain the single composite EVI for the PBTC. Here we consider the maximum months (January–March) of observed imagery in a preceding year as the base year in the order of 1990, 1995, 2000, 2005, 2010, 2015, and 2018.

2.3. Forest Land Cover Category Threshold Values

In our previous study [24], we were able to determine the major land cover category threshold values, which were derived by assessing phenological characteristics of land cover categories during the mid-dry phenological season (December to March) using the GEE harmonic model function for Landsat TM and Landsat OLI EVI time series data as described in our previous paper [24]. The phenology-based threshold values for individual land cover categories were set for the Landsat 5 (1990–2010) and Landsat 8 (2015–2018) median EVI data. These land cover category threshold values can be applied to the Landsat 5 and Landsat OLI EVI data to classify the forest land cover categories in tropical regions, such as Cambodia. A detailed description of EVI land cover category phenology assessment can be found in our previous paper [24].

Phenology-based threshold values were applied to seven forest categories and three non-forest categories (Croplands, Water and other land cover) in the mid-leaf-shedding phase by selecting their high-peak vegetation index values in this study [24]. The selected forest land cover category threshold values are presented in Table 2 and the JavaScript used for PBTC is available at [24].

In our previous study [24], the EVI vegetation index values of the Flooded forest were difficult to determine because they were similar to the those of the other forests, specifically Evergreen and Semi-Evergreen forest (Table 2) during the mid-dry phenological season. To avoid this confusion, we created a boundary around the Tonle Sap lake for the Flooded forest area in GEE using the geometry tool, and then separately assigned the threshold values (TM: 0.381–0.519 and OLI: 0.382–0.581) in both Landsat TM and Landsat OLI collections to avoid misclassification and improve the map accuracy.

Table 2. EVI threshold values used for forest land cover change detection in the Siem Reap province, Cambodia, using Landsat Collections.

Forest Land Cover Categories in This Study	TM Threshold Values (1990–2010)		OLI Threshold Values (2015–2019)	
	Min	**Max**	**Min**	**Max**
Bamboo	0.671	0.776	0.854	0.882
Plantation (Rubber)	0.659	0.661	0.815	0.841
Evergreen	0.515	0.659	0.652	0.769
Semi-Evergreen	0.435	0.501	0.581	0.648
Deciduous	0.301	0.421	0.476	0.556
Mixed woods and shrubs	0.212	0.275	0.385	0.445
Flooded forest	0.381	0.519	0.382	0.581

Note: TM Landsat Thematic Mapper 5; OLI Landsat Operational Land Imager 8; and Min and Max are the forest cover categories' mean EVI threshold values [24].

2.4. Phenology-based Threshold Classification

The Google Earth Engine offers a range of image processing approaches such as the compute images at-sensor radiance, TOA reflectance, cloud score and cloud-free composites [37]. We applied JavaScript algorithms to the entire Landsat collections, converted these to median values, and then applied a cloud thrash/mask function to obtain a cloud-free image. Finally, we applied a filter collection function to limit the image to those pixels within the Siem Reap province between December and March in each year. We applied the GEE PBTC algorithms for a composite EVI for forest land cover and carbon stock changes in the study region, which involved five steps (Figure 2):

1. Landsat TM and Landsat OLI TOA collections were accessed using an image collection function in GEE and then a filter function was applied to obtain the collections for a specific season. We used the Siem Reap province area boundary to filter the collections within the study region.
2. We used a cloud mask function to minimize the cloud cover on the image to less than 60%, and applied reducer functions to reduce the median values per pixel [50]. The reducer functions decrease the dimensionality of image collections by calculating simple statistics, such as the median value for each pixel. The output reducer median image object (single raster layer) characterizes the quality of the complete image collection.
3. The EVI function for the median Landsat collections were applied to entire image collections from 1990 to 2018 [24,51,52].
4. We assigned the phenology-based threshold values for individual land cover categories by referring to our previous study [24] and then applied the PBTC function in GEE for the forest land cover classification. The resulting maps were validated using very high-resolution images (VHR) in Google Earth-Pro time-lapse.
5. We assessed the forest cover changes from the PBTC maps and calculated the carbon stock changes and emissions by applying equations adapted from Good Practice Guidelines of the Intergovernmental Panel on Climate Change [53] and Sasaki et al. (2016) [10] over the 28-year period. Finally, we established the subnational FREL (using the retrospective approach) up to 2030, an upcoming milestone under the Paris Agreement to which Cambodia is a signatory country.
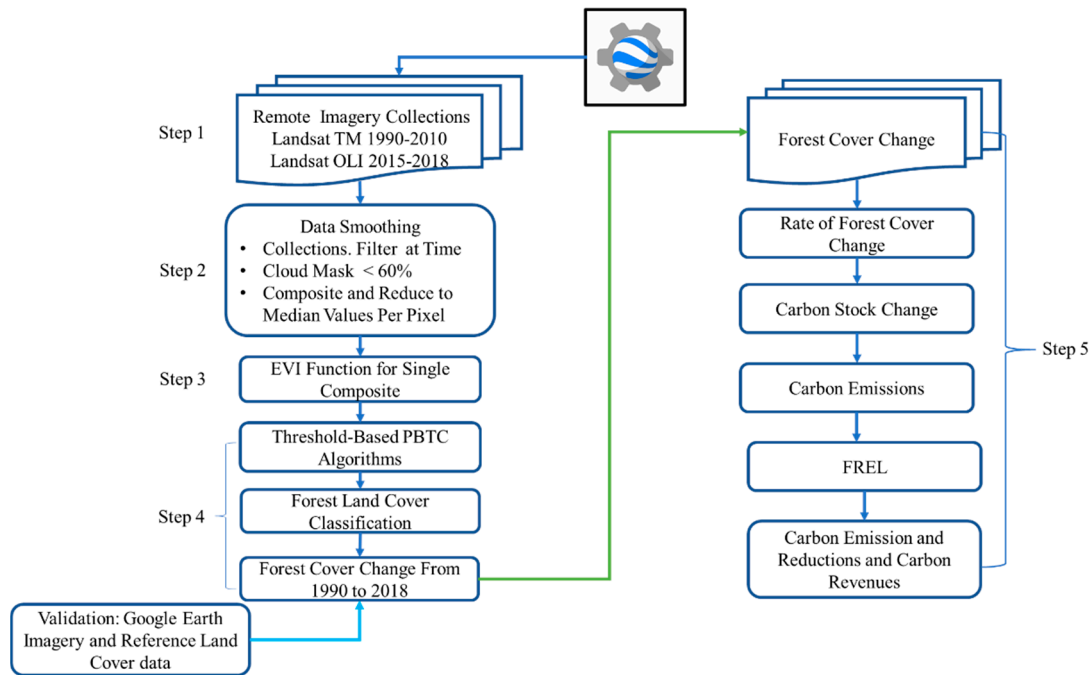
Figure 2. PBTC methodology in Google Earth Engine for land cover mapping in Siem Reap province, Cambodia.

2.5. Accuracy Assessment and Data for Validation

Google Earth is highly detailed digital representation of the globe and has recently been recognized for its potential to significantly improve the visualization of land use land cover change science. Higher resolution imagery from Google Earth is free of charge and can be used directly in land use land cover map validation at any scale [54]. The images are constantly updated when new data become available. Depending on the sensor, imagery resolution ranges from 30 m to 15 cm. Utilizing the time-lapse feature in Google Earth provides access to zoomable images as far back as 30 years, which are ideal for monitoring land use land cover changes [55]. Furthermore, it is powerful source of location intelligence data that can be used for investigation and preliminary studies with suitable accuracy [56,57].

Google Earth VHR time series imagery can be used to assess the accuracy of reference data. This accuracy can be enhanced by applying recognized protocols as recommended by Olofsson et al. [58]. In this study, systematic centric sampling techniques were employed to obtain the reference data for validating the PBTC maps (Figure 3). A total of 419 samples of 5 × 5 km Universal Transverse Mercator coordinate system (UTM) grid points were established for each PBTC map in 1990, 1995, 2000, 2005, 2010, 2015 and 2018 (Figure 3A). The existing available land cover reference data in 2002 and 2006 from Sasaki et al. [10] were used to validate the PBTC 2000 and 2005 maps (Figure 3B).
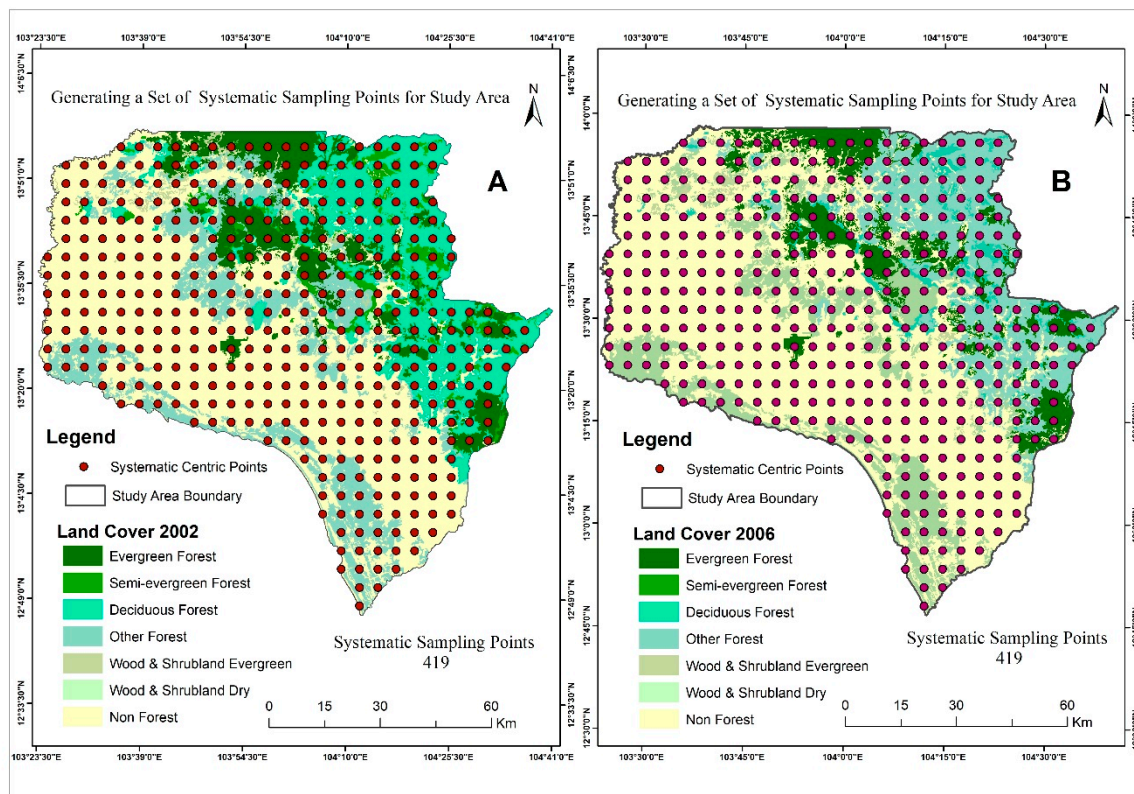
Figure 3. Map showing the systematic (5 × 5 km) centric sampling points using Esri's ArcMap for PBTC map (**A**) and reference land cover map (**B**) [10,59].

Using the ArcMap Fishnet tool, the systematic centric points were allocated to the respective points for accuracy assessment on the forest land cover maps within the study region. For any point in the sample, we manually assessed whether the point fell on a certain land cover category however, consideration of the size of the forest land cover category was not required. A total of 3771 reference points were spatially established, of which 2933 were for seven PBTC maps (1990–2018) and 838 were for the two reference land use land cover maps (2000 and 2005).

Subsequently, the PBTC maps were exported to Google Drive using the export function in GEE for accuracy validation. We used these maps in ArcMap to transform land use labels into 3771 points for validation using ArcMap spatial-join and related tools. The generated 5 × 5 km systematic centric sampling points were then converted into a "kml" file and imported into Google Earth for validating the PBTC maps.

All of the 3771 sampling points were visually analyzed using the Google Earth "time slider" tool to compare and validate the PBTC land cover categories with historic images from 1990 to 2018. This procedure enabled the verification and validation of the proximate PBTC land cover category with great accuracy and reliability because computation could be executed on a point-by-point basis (Figure 4).

The reference land cover maps (2000 and 2006) were classified into seven classes: Evergreen forest (EG), Semi-evergreen forest (SE), Deciduous forest (DD), Wood and shrub evergreen (WE), Wood and shrub dry (WD), Other forest (OF) and Non forest (NF). To validate the PBTC map accuracy of the maps in 2000 and 2005, we combined PBTC land cover categories as follows: Water (WA), Others (OT) and Croplands (CR) were merged into the NF category; Flooded forest (FF) and Bamboo (BB) were merged into the OF category; and WE and WD were merged into the Mixed WS. The EG, SE and DD categories were unchanged. Furthermore, the generated 5 × 5 km 838 spatial reference sample points were visually analyzed to compare and validate the PBTC land cover classes in 2000 and 2005 using reference land cover data in 2002 and 2006.

Figure 4. Maps showing the locations of accuracy points for accuracy assessment using Google Earth high-resolution imagery. These points were used to verify and validate the PBTC land cover categories, namely, the Evergreen forest (EG), Semi-Evergreen forest (SE), Deciduous forest (DD), Mixed woods and shrubs (WS), Bamboo (BB), Flooded forest (FF), Rubber plantation (RB), and Croplands (CR).

We then calculated the producer's accuracy (PA) by dividing the number of 5×5 km accuracy points in an individual land cover category identified accurately by the respective reference points total. The user's accuracy (UA) was computed by dividing the number of reference points in an individual land cover category identified accurately by the classified total. Finally, the overall classification accuracy (OA) was derived by dividing the total number of accurately classified land cover categories by the total number of reference points, and the Kappa coefficient (K) of agreements was calculated [23,24,58,60] for the PBTC maps and reference land cover maps using a confusion matrix.

2.6. Carbon Stocks and Emission Reductions

To implement the REDD+ scheme, Cambodia employs a national definition of forest consistent with the Global Forest Resources Assessment [59], which is part of the Intergovernmental Panel on Climate Change (IPCC) "FOREST" land use category (Table 3).

Sasaki et al. [10], estimated above-ground biomass, below-ground biomass, deadwood, litter, and total carbon stocks in seven forest categories (Evergreen Forest, Semi-Evergreen, Deciduous Forest, Bamboo, Other forest, Wood Shrubland Dry and Wood Shrubland Evergreen) and estimated FREL at a provincial level using a retrospective approach. Here, we focused only on major forest categories and rubber plantations. For Mixed woods and shrubs carbon density, we used the average total carbon stocks (39.45 MgC/ha) of Wood Shrubland Dry and Wood Shrubland Evergreen. The weighted average (MgC/ha) was calculated only for Siem Reap Province using 1990 forest cover carbon stocks as a baseline (Table 3).

We used the formulas below for calculating the carbon stocks and emission reduction in seven forest categories, namely: Evergreen, Semi-evergreen, Deciduous, Mixed Woods and Shrubs, Bamboo, Flooded Forest, and Rubber Plantation. We estimated total forest area carbon stocks (*CS*) and summed carbon stocks from all four pools using forest categories as reported in [10].

Table 3. Selected forest land use categories and initial carbon density for Siem Reap province.

IPCC Land Use Category	Forest Land Cover Categories	Initial Carbon Density (MgC/ha)				Total Carbon Stocks	
		Above Ground	Below Ground	Dead Wood	Litter	(MgC/ha)	(MgCO$_2$)
FOREST	Evergreen Forest	96.2	27.8	27.2	13.6	164.8	604.27
	Semi-Evergreen	98.1	29.8	14.5	12.4	154.8	567.60
	Deciduous Forest	95.1	28.9	14.1	12	150.1	550.37
	Bamboo	36.4	11.1	5.4	4.6	57.5	210.83
	Flooded Forest	32.9	9.5	9.3	4.7	56.4	206.80
	Rubber Plantation	47	13.6	13.3	6.6	80.5	295.17
	Wood Shrubland Dry	20	6.1	3	2.5	31.6	115.87
	Wood Shrubland Evergreen	30	9.1	4.4	3.8	47.3	173.43
	Weighted Average of Total Carbon Stocks					121.6	445.9

Note: Adapted initial carbon pools for forest land use categories were obtained from Sasaki et al. (2016) [10] and the initial forest reference level for Cambodia under the UNFCCC [59].

2.6.1. Estimating the Forest Land Cover Change

The retrospective approach was used to develop forest cover changes based on past deforestation trends for the province by applying Equation (1) [10].

$$FA_i(t) = FA_i(0) \times e^{a_i \times t} \tag{1}$$

where $FA_i(t)$ is the total forest cover (ha) of each forest land category (i) at time t (year), FA_i (0) is the forest cover (ha) of forest land cover category (i) at the start of the model (0) (i.e., in 1990), a_i is the rate of change of each forest land cover category i between 1990 and 2018. Using data in Table 4, a_i was derived for each forest land cover category between 1990 and 2018. a_i and FA_i (0) were obtained from regression analysis using the PBTC data from 1990, 1995, 2000, 2005, 2010, 2015 and 2018. Using this a_i value, forest cover and change between 1990 and 2030 were estimated.

Table 4. Forest land cover change rate by category from the regression analysis.

Forest Category i	a_i	Initial Values of Forest Area$_i$ (t0)	R^2
Mix Woods and Shrubs	−0.02	151,201.84	0.48
Deciduous Forest	−0.01	253,342.02	0.73
Semi-Evergreen Forest	−0.01	253,342.02	0.73
Evergreen Forest	−0.01	209,323.64	0.84
Flooded Forest	−0.02	153,747.99	0.92

2.6.2. Estimation of Total Forest Carbon Stocks

Total forest carbon stocks in Siem Reap province between 1990 and 2018 were obtained by:

$$TCS(t) = \sum_{i-1}^{7} FA_i(t) \times CS_i \tag{2}$$

where *TCS(t)* is total above ground carbon stocks in Siem Reap province (MgC); FA_i is the area of the 7 forest categories $_i$ in the province of 12 districts; CS_i is the carbon stocks (MgC/ha/year) in 7 forest categories $_i$.

2.6.3. Annual Carbon Emissions Due to Forest Cover Change

The Gain–Loss method was applied to obtain carbon emissions by forest category using Equation (3):

$$CE\ (t) \frac{\sum_{i=1}^{5}[FA_i(t_2) - FA_i(t_1)] \times CS_i}{t2 - t1} \times \frac{44}{12} \tag{3}$$

where, *CE* (*t*) = annual carbon emissions (MgCO$_2$/year (*t*)) due to deforestation in Siem Reap province. CS_i is the average of carbon stocks for forest category *i* (MgC/ha) in Table 4. We excluded the Bamboo and Rubber plantation categories in the projected carbon emissions because their combined total forest land cover area and carbon stocks are less than 10% of total carbon stocks. Therefore, these two forest categories can be ignored as per IPCC guidelines [53]. The ratio 44/12 is the molecular weight ratio of carbon dioxide to carbon [10,53].

2.6.4. Forest Reference Emission Level between 2020 and 2030

The FREL is an essential benchmark for carbon emissions. The more countries agree to reduce emissions, the more financial support they receive according to REDD+ schemes for performance-based payments [61]. However, it is important to have a good understanding of the historical trend of land use and land cover change and forest deforestation at a moderate to high resolution scale because this helps to establish FREL for measuring the performance when the REDD+ activities are implemented. FREL can be established by:

$$FREL\ (t) = CE(t) \tag{4}$$

where *FREL*(*t*) = Forest reference emission level in Siem Reap at time *t* (MgCO$_2$/year). Because we used the retrospective approach, *FREL* for Siem Reap province during the Paris Agreement (2020–2030) is the same as the projected *CE*(*t*) during the same period between 2020 and 2030.

2.6.5. Project Emissions

If REDD+ project is implemented to reduce the deforestation and forest degradation in the Siem Reap province, the emissions from such project can be estimated by:

$$PE(t) = FREL(\text{t}) \times [1 - RPI(\text{t})] \tag{5}$$

where *PE*(*t*) **=** Project emission (MgCO$_2$/year); *RPI*(*t*) is relative project impact taken from Ty et al. [62].

2.6.6. Emission Reductions

Accordingly, carbon emission reductions can be obtained by:

$$ER(t) = FREL(t) - PE(t) \tag{6}$$

where *ER*(*t*) is annual emission reduction (MgCO$_2$/year) at time *t* between 2020 and 2030

2.6.7. Carbon Revenues

$$CR(t) = ER(t) \times CP \tag{7}$$

where: *CR* is carbon revenues from emission reduction (MgCO$_2$/year) in Siem Reap province between 2020 and 2030; *CP* is the carbon price of USD 7 per MgCO$_2$ reported in World Bank and Ecofys [63].

3. Results

3.1. PBTC Land Cover Map Accuracy

The GEE PBTC maps were shown to be more accurate according to the confusion matrix estimated in this study. The details of the forest land cover category's overall accuracies (OA), Kappa coefficients (K), producer's accuracies (PA) and user accuracies (UA) of the maps are presented in Tables 5 and 6. Appendix A (Tables A1–A7) shows the PBTC map accuracy matrix and reference map accuracy matrix.

Table 5. Classification accuracy (%) for PBTC maps using Google Earth high-resolution imagery from 1990 to 2018.

Land Cover Categories	1990 UA	PA	1995 UA	PA	2000 UA	PA	2005 UA	PA	2010 UA	PA	2015 UA	PA	2018 UA	PA
Water	100	100	100	100	100	82	100	77	100	83	100	86	100	100
Others	78	100	80	50	64	58	45	100	78	93	65	85	64	100
Croplands	100	95	92	97	90	88	98	97	99	91	94	94	96	94
Mixed Woods and Shrubs	98	90	91	93	82	84	92	85	84	86	82	61	86	67
Deciduous Forest	93	95	97	90	95	99	88	97	92	96	77	96	82	96
Evergreen Forest	84	89	87	85	95	92	98	82	92	91	97	86	92	90
Semi-Evergreen Forest	91	87	86	98	90	96	91	97	82	89	88	96	86	95
Rubber Plantation											100	50	50	50
Bamboo	60	100	100	100	100	67	75	100	67	67	60	60	75	50
Flooded Forest	100	100	100	100	100	100	100	100	98	100	98	98	96	100
Overall Accuracy (%)	92.84		92.6		92.12		92.84		91.89		89.5		90.93	
Kappa	0.91		0.91		0.91		0.91		0.90		0.87		0.88	

Note: PA represents producer's accuracy, UA is user accuracy, OA is overall classification accuracy, and K is Kappa coefficients.

Table 6. Classification accuracy (%) for PBTC maps using reference land cover data in 2000 and 2005.

Land Cover Categories	2000		2005	
	UA	PA	UA	PA
Evergreen Forest	92	86	81	76
Semi-Evergreen Forest	89	75	90	70
Deciduous Forest	82	73	77	76
Mixed Woods and Shrubs	80	65	84	58
Other Forest	65	76	83	86
Non-Forest	82	96	84	98
Overall Accuracy (%)	81.38		83.05	
Kappa	0.77		0.78	

The overall classification of accuracy of the GEE PBTC maps for 1990, 1995, 2000, 2005, 2010, 2015, and 2018 was 92.84%, 92.6%, 92.12%, 92.84%, 91.89%, 89.5% and 90.93%, respectively. The overall K statistics were 0.91, 0.91, 0.91, 0.91, 0.90, 0.87 and 0.88 (Table 5). The overall cumulative accuracy of this study was 92.1% and its K statistic was 0.9. Generally, the results of PBTC map accuracy are acceptable as suggested by the United States geological survey satellite imagery classification schema [64]. K statistics results greater than 0.85 represent stronger agreements between the classification made and the Google Earth imagery validation information [65]. By comparison, the overall accuracy of the reference maps was 81.38% in 2000 and 83.05% in 2005, and the K statistic for 2000 was 0.77, and that for 2005 was 0.78 (Table 6), which is acceptable.
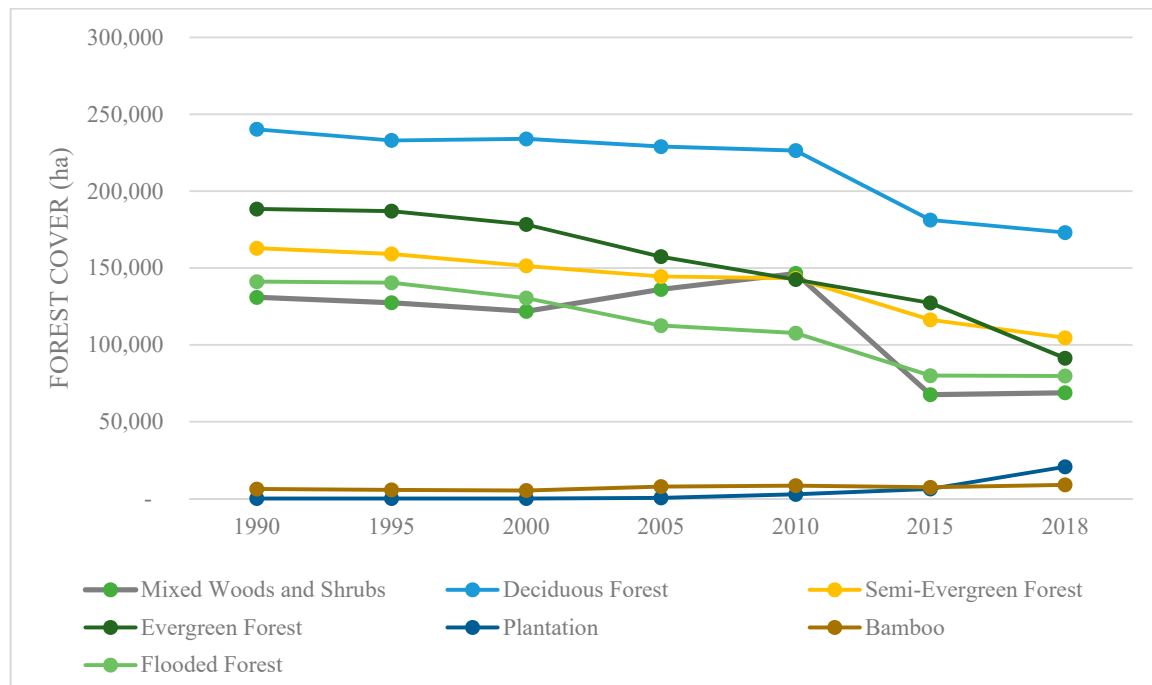
3.2. Siem Reap Forest Cover Change

The PBTC maps between 1990, 1995, 2000, 2005 and 2010 (Figure 5A–E) were derived from Landsat TM and Landsat OLI from 2015 and 2018 (Figure 5F,G), and show the geographic distribution of forest category land cover in Siem Reap Province. The major types of forest are found in Siem Reap province: Evergreen forest, Semi-Evergreen forest, Deciduous forest, Mixed woods and shrubs, Flooded forest, and Bamboo. Our findings show that the Deciduous forest covers a larger area than other forest, followed by Semi-Evergreen and then Evergreen forest. The Evergreen and Semi-Evergreen are forests largely found in north and northeastern districts, protected areas and the Angkor wat temple surroundings. The Flooded forest was found adjacent to the Tonle Sap lake and the southern part of the region. Bamboo distribution was found in elevated regions in the most northern part and was mixed with Evergreen and Semi-Evergreen forests in the Banteay Srei, Varin, Svay Leu, Angkor Chum,

and Chi Kraeng districts. The expansion of Rubber plantations can be seen in the Chi Kraeng and Varin districts (Figure 5G). The mixed woods and shrubs category was distributed with Deciduous forest and close to Croplands (Figure 5).
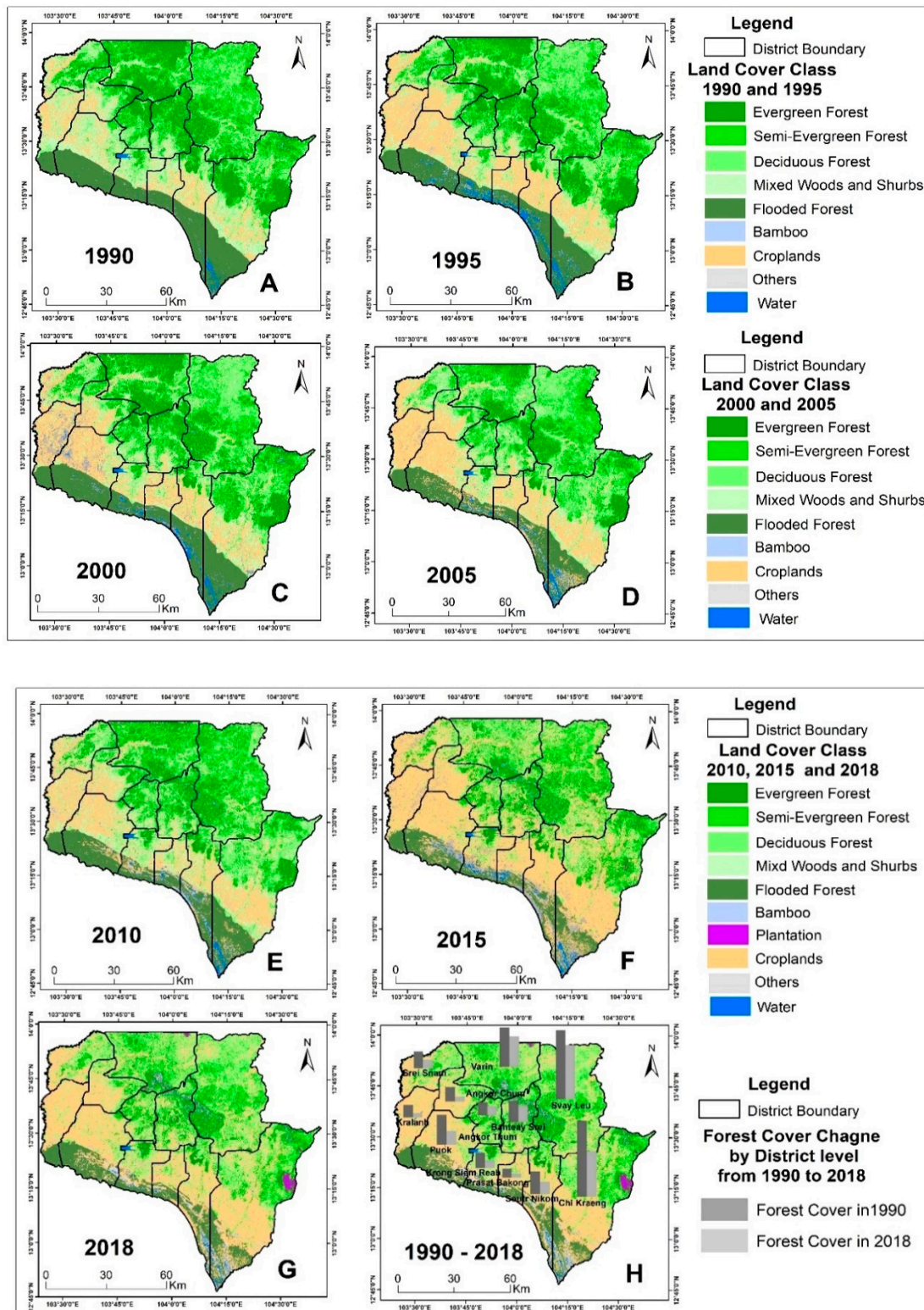
Figure 5. Land cover in Siem Reap province in 1990 (**A**), 1995 (**B**), 2000 (**C**), and 2005 (**D**), 2010 (**E**), 2015 (**F**), and 2018 (**G**), and forest cover change at the district level between 1990 and 2018 (**H**). The graph on the map (Figure 5H) shows the forest cover in 1990 (dark color) and in 2018 (light dark color).

The Siem Reap province forest area gradually decreased from 1990 to 2000. A significant reduction can be seen from 2010 to 2015 (Figure 6). See Appendix A, Table A10 for forest category land cover change in Siem Reap province from 1990 to 2018.


Figure 6. Trend of forest land cover change in Siem Reap province from 1990 to 2018.

Among the seven main forest categories, the annual change in Evergreen forest was 3467 ha. The rate of decrease was 1.8% from 1990 to 2018; Semi-Evergreen forest decreased at the rate of 1.3% and Deciduous forest decreased at 1.0% over the 28-year period. The Mixed woods and shrubs forest area showed the second highest rate of decrease compared to other forest categories (1.7%). Flooded forest areas experienced substantial losses of 61,420 ha annually at a rate of 1.6%. The province's forest area decreased by 322,694 ha in all forest types with an average annual rate decline of 1.3% over a 28-year period (1990–2018). A rapid decline in forest cover was observed between 2010 and 2018 and a slight increase in the Rubber plantation and Bamboo forest cover can be noted during the same period (Figure 6 and Appendix A, Table A10).

3.3. Changes in Carbon Stocks by Forest Category

Using the GEE PBTC maps, we were able to calculate the forest carbon stocks (MgC) from 1990 and 2018 (Figure 7).

In 1990, most carbon stocks were concentrated in deciduous forests, totaling 36,030,716 MgC; Evergreen forest stocks were 31,037,040 MgC, and Semi-evergreen forest 25,217,307 MgC. In 2018, the changes in forest carbon stocks represent the highest concentrations of carbon stocks from the Deciduous forest of 25,951,554 MgC. Semi-Evergreen forest was 16,191,616 MgC, Evergreen forest 15,038,590 MgC, Flooded forest 4,492,959 MgC, and the Rubber plantation carbon stocks increased from 215,479 MgC to 1,662,963 MgC between 2010 and 2018. Overall, 39,198,938 MgC of forest carbon stocks were lost in the province during the past 28 years (Table 7).
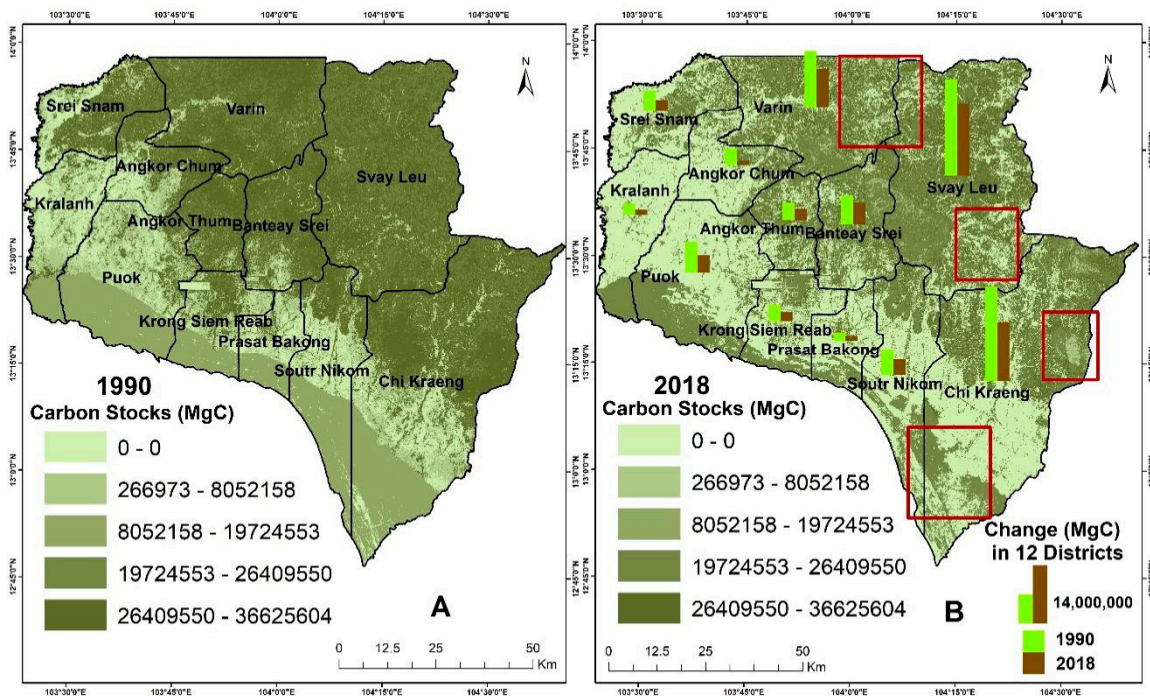
Figure 7. Carbon stock in 1990 and 2018 in Siem Reap province. (**A**) Map of spatial carbon stock (MgC) concentrations in 1990 and (**B**) map showing the spatial carbon stock concentrations in 2018. The red boxes indicate the larger changes of carbon stocks (MgC) in the region. Note: 0 (Mgc) falls within the non-forest areas including water and other land cover category. The graph on the map (Figure 7B) shows the carbon stock change from 1990 (light green color bars) to 2018 (dark brown color bars) and 14,000,000 is the scale of the bar graph.

Table 7. Changes in forest carbon stocks by forest category.

Forest Categories	Total Forest Carbon Stocks (MgC)							Change
	1990	1995	2000	2005	2010	2015	2018	1990–2018
Evergreen forest	31,037,040	30,804,960	29,375,355	25,931,242	23,475,922	20,969,205	15,038,590	−15,998,450
Semi-Evergreen forest	25,217,307	24,642,090	23,440,265	22,372,222	22,184,966	18,007,231	16,191,616	−9,025,690
Deciduous forest	36,030,716	34,946,363	35,091,036	34,341,517	33,949,707	27,172,999	25,951,554	−10,079,162
Mixed woods and shrubs	5,163,076	5,024,348	4,803,599	5,367,776	5,776,749	2,665,304	2,713,442	−2,449,634
Flooded forest	7,957,072	7,914,681	7,355,401	6,345,094	6,069,433	4,510,094	4,492,959	−3,464,113
Bamboo	353,690	321,444	299,083	445,896	480,099	417,636	508,837	+155,147
Rubber plantation	0	0	0	0	215,479	500,590	1,662,963	+1,662,963
Total (MgC)	105,758,901	103,653,886	100,364,739	94,803,748	92,152,354	74,243,060	66,559,963	−39,198,938

Note (+) represents an increasing trend of Rubber plantation and Bamboo cover and their carbon stocks in Siem Reap province.

3.4. Forest Cover and Carbon Stock Changes and Carbon Loss

Chi Kraeng District had the most forest area in the province; however, 35% was deforested between 1990 and 2018 (81,548 ha). Svay Leu District was the second most forested district (189,826 ha in 1990) and it also lost 35% by 2018. Over the same period, Krong Siem Reap lost 38%, Angkor Chum 37%, Srei Snam 35%, Soutr Nikom 35% and Angkor Thum 30%. These 12 districts accounted for 31% of the total deforestation in Siem Reap province between 1990 and 2018. Fifty-two percent of the province remains forested, mostly in Chi Kraeng, Svay Leu, Puok and Varin Districts. Table 8 presents the district level forest cover changes during the past 28 years.

Table 8. District level forest land cover change.

| District Name | District Area (ha) | Forest Area Cover (ha) | | | | | | | Change | Forest Area Loss |
		1990	1995	2000	2005	2010	2015	2018	1990–2018	(% of District Area)
Angkor Chum	47,903	34,695	32,819	30,687	29,479	28,081	17,513	16,794	−17,901	37%
Angkor Thum	35,725	35,252	35,103	34,504	33,909	33,802	25,782	24,671	−10,581	30%
Banteay Srei	60,070	58,117	58,031	56,208	55,100	55,487	46,050	46,099	−12,018	20%
Chi Kraeng	236,236	207,124	203,086	196,058	178,956	177,110	123,162	125,576	−81,548	35%
Kralanh	56,807	19,060	18,632	15,225	14,492	14,359	11,114	11,323	−7,737	14%
Puok	101,170	59,837	56,720	52,958	49,897	52,886	37,876	36,267	−23,571	23%
Prasat Bakong	34,174	18,867	18,753	17,201	16,180	18,169	9,353	9,678	−9,190	27%
Krong Siem Reab	47,064	39,112	35,005	30,928	28,983	31,442	19,500	21,217	−17,895	38%
Soutr Nikom	77,961	60,724	59,665	55,646	50,984	48,461	29,465	33,127	−27,598	35%
Srei Snam	55,757	39,659	39,535	39,182	38,693	37,655	21,500	20,293	−19,366	35%
Svay Leu	191,769	189,826	188,964	187,312	188,055	183,466	156,980	123,326	−66,499	35%
Varin	109,833	107,181	105,961	104,995	102,719	96,171	87,372	78,389	−28,792	26%
Total Forest Area (ha)		869,455	852,274	820,904	787,447	777,091	585,667	546,760	−322,695	31%

In 1990, total carbon stocks in seven forest categories were estimated to be 105,758,901 MgC and in 2018, 66,559,963 MgC, in 12 districts (Table 9). In all districts from 1990 to 2018, the total carbon stocks decreased by 39,198,938 MgC and were responsible for annual carbon emissions of 143,729,440 MgCO$_2$ over the 28-year period. Over the same period, Svay Leu District emitted 39,719,781 MgCO$_2$, followed by Chi Kraeng District with 33,792,193 MgCO$_2$. These figures are for four IPCC total carbon pools, including above ground, below ground, litter, and deadwood. However, estimated overall emissions vary depending on the methods used to calculate them (Table 9).

Table 9. District level forest carbon stock (MgC) changes and baseline emissions (MgCO$_2$).

| District Name | Carbon Stock (MgC) | | | | | | | Change (MgC) | Baseline Emissions (MgCO$_2$) |
	1990	1995	2000	2005	2010	2015	2018	1990–2018	1990–2018
Angkor Chum	4,481,724	4,211,397	3,911,139	3,408,585	3,251,072	2,315,103	2,135,163	−2,346,560	8,604,055
Angkor Thum	4,855,619	4,839,508	4,771,925	4,568,961	4,395,144	3,615,001	3,339,834	−1,515,785	5,557,879
Banteay Srei	8,262,586	8,249,766	7,905,274	7,303,403	7,115,624	6,364,061	6,184,869	−2,077,717	7,618,294
Chi Kraeng	24,488,598	23,963,522	22,949,721	20,712,337	20,007,740	15,403,953	15,272,545	−9,216,053	33,792,193
Kralanh	1,181,106	1,124,929	947,458	865,618	853,668	714,529	777,719	−403,387	1,479,087
Puok	4,018,699	3,612,435	3,426,130	3,165,192	3,316,049	2,595,245	2,493,081	−1,525,618	5,593,934
Prasat Bakong	1,315,828	1,299,782	1,186,309	1,092,475	1,317,564	790,736	854,862	−460,965	1,690,207
Krong Siem Reab	3,370,934	2,846,418	2,502,309	2,366,718	2,792,187	2,089,725	2,244,190	−1,126,744	4,131,395
Soutr Nikom	5,558,495	5,500,495	5,246,731	4,834,828	4,530,883	3,004,410	3,466,244	−2,092,251	7,671,587
Srei Snam	4,902,947	4,923,917	4,817,213	4,436,199	4,308,653	2,783,376	2,469,911	−2,433,036	8,921,130
Svay Leu	27,432,714	27,341,797	27,124,702	27,075,938	26,315,551	22,401,760	16,600,047	−10,832,667	39,719,781
Varin	15,889,651	15,739,920	15,575,828	14,973,492	13,948,221	12,165,160	10,721,497	−5,168,154	18,949,900
Total (MgC)	105,758,901	103,653,886	100,364,739	94,803,748	92,152,354	74,243,060	66,559,963	−39,198,938	143,729,440

3.5. Carbon Emission, FREL and Emission Reductions

The total FREL for Siem Reap province was estimated to be 35,303,937 MgCO$_2$ and the project emission reduction to be 8,256,746 MgCO$_2$ for the 10-year project period from 2020 to 2030. If REDD+ activities are initiated in Siem Reap province to maintain the existing forest, the province has the potential to receive carbon revenues of about USD 57.8 million during the project period from 2020 to 2030 (Appendix A, Table A11). However, the carbon price (USD7/MgCO$_2$) can vary depending on international negotiations with emission trading and carbon offset schemes [63].

4. Discussions and Implications

Our study found that the PBTC mapping accuracy (Tables A1–A7) is higher than that of previous studies in the region (FREL, 2016) and our results show a significant decrease in forested land in Siem Reap province from 1990 to 2018 (Table A10). Although nearly half of the province is still covered in forest, the quality and value of forest ecosystems has generally declined by about 31% or 322,694 ha in 28 years (Table 8). This decline can be attributed to forest clearing to accommodate an

increase in population and new households [66], expansion of Croplands [67], and the government's Economic Land Concession program to promote plantations [68]. Other major drivers of deforestation and degradation were the expansion of agriculture to grow cassava, orchard plantations, and paddy fields [16,47]. Evergreen, semi-evergreen, and deciduous forests have been subjected to logging [59]. The flooded forests and floodplains that surround the Tonle Sap fresh water lake provide shelter for fish to breed in addition to important feeding areas. The flooded forest area declined from 141,083 ha to 76,662 ha from 1990 to 2018 (Table A10). The main reason could be the use of smoke to harvest honey, burning firewood, and leaving cooking fires unattended. In addition, farmers may have burned flooded forests for conversion to rice growing, hunting animals, or setting long fishing nets across river channels [69]. Between 2010 and 2018, most districts lost forest cover as a result of rapid population growth, tourism, and the need for land for agricultural production [66]. The main factors affecting carbon stock changes were deforestation, expansion of croplands, and economic land concessions in the region [66]. Chi Kraeng and Svay Leu district forest lands have been converted to plantations, croplands, and economic land concessions, which may be the cause of high concentrations of emissions (MgCO2) in both districts. Due to forest deforestation, the province lost 39,198,938 (MgC) carbon stocks over all forest types between 1990 and 2018 or about 143,729,440 $MgCO_2$ of total carbon emissions over the same period (Table 9).

Previous studies showed the rate of deforestation in the province to be 2.6% between 2002 and 2006 [10], which is higher than our result. This could be due to a lack of long-term temporal data, as the previous study used activity data from only two time periods (2002 and 2006), during which forest cover sharply declined during the same period [66]. It is generally the case that the more time series activity data available, the better the resulting relationship for estimating FREL [61]. Nevertheless, both of the predicted linear trends show similar fitted values (R^2 = 0.97) of projected FREL from 2020 to 2030. As seen in Figure 8, total FRELs were estimated to be 20,431,376 $MgCO_2$ for 10 years from 2020 to 2030, which is higher than that projected by Sasaki et al. [10] (Figure 9).
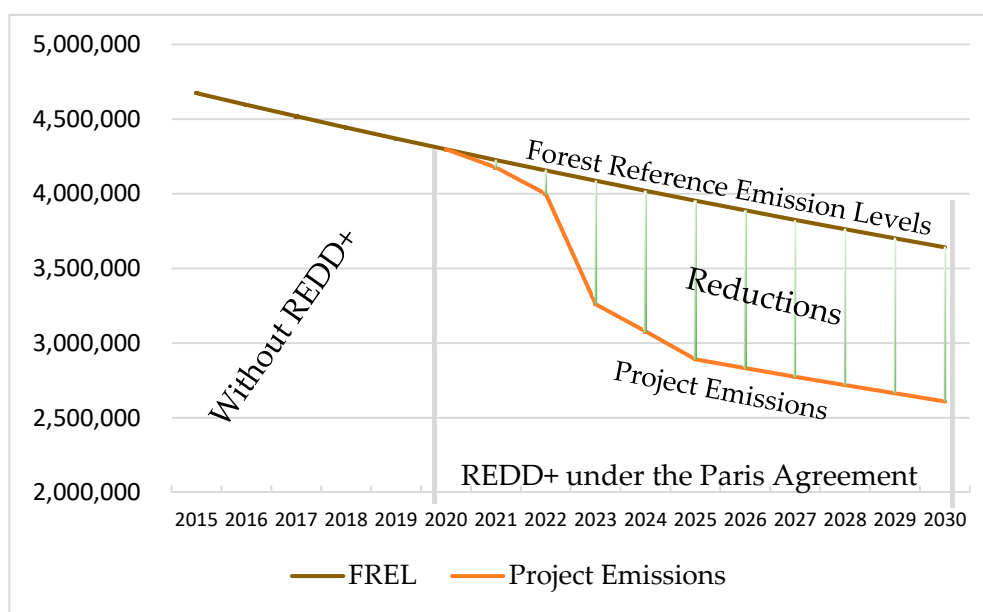
Figure 8. Forest reference emission levels and emission reductions in Siem Reap province during a 10-year project period (2020–2030). See Appendix A, Table A11 for total Forest reference emission levels (FREL) for Siem Reap province from 1990 to 2030.
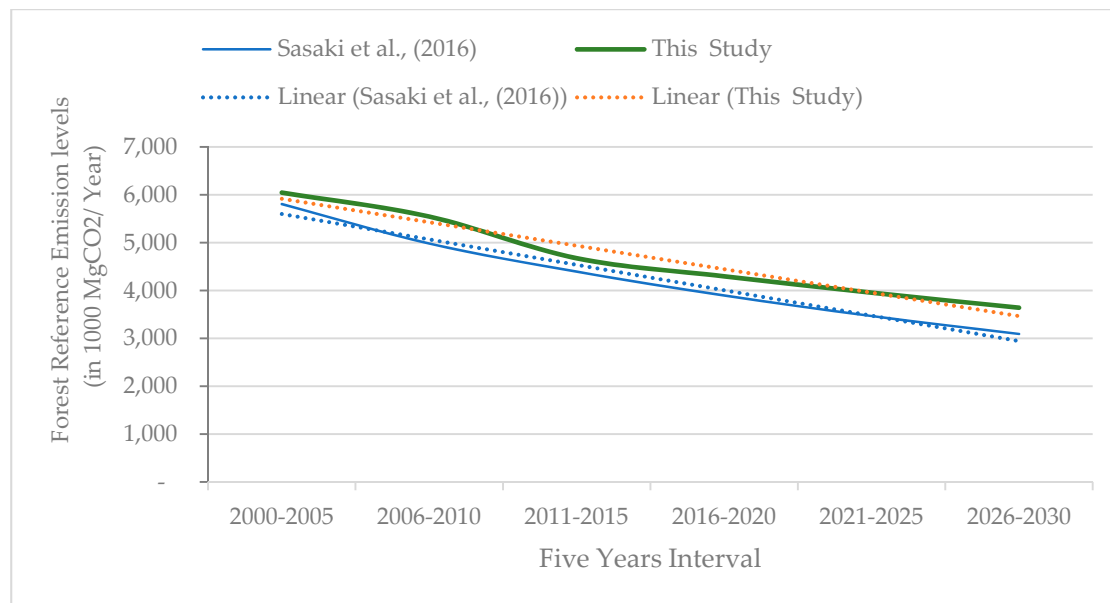
Figure 9. Validation of annual forest reference emission levels. Linear fitted line for this study: $y = -490.71 * x + 6410.4$, $R^2 = 0.9651$. Linear fitting line for Sasaki et al. [10]: $y = -531.82 * x + 6133.8$, $R^2 = 0.9793$.

REDD+ monetary incentive payments result from the amount of accountable carbon credits and the price paid per ton of carbon. Carbon emission reduction prices rose between 2017 and 2018; for example, the European Union Allowance fee rose from USD7/MgCO$_2$ to USD16/ MgCO$_2$ between 2017 and 2018. However, carbon emission reduction prices range widely between initiatives, from less than USD1/MgCO$_2$ (Mexico, Poland and Ukraine carbon tax) to a maximum USD 139/MgCO$_2$ (Sweden carbon tax) [63]. The REDD+ scheme offers financial incentives for reducing emissions or increasing removals or carbon sequestration in forest and agricultural lands [70–73]. Carbon revenue is dependent on carbon prices. If the carbon price of USD16 is used, the total carbon revenue is USD132.11 million. On the other hand, if the price used is the same as that of Sweden, then the total revenue would be USD1147.69 million at the time of the Paris Climate Agreement between 2020 and 2030. Because the number of sustainability travelers has increased by about 48% [74], the REDD+ project site could become a tourist destination, thereby generating more revenue for local people.

Our study map accuracy shows that the Mixed woods and shrubs category is the main source of confusion in the Deciduous forest and Semi-Evergreen forest. The Semi-Evergreen forest is the main source of confusion in the Evergreen forest category in all the classified years (1990 to 2018). Flooded forest improved the accuracy of PA and UA because the Flooded forest was mapped separately by creating the Flooded forest boundary. In contrast, the Water, Bamboo, Rubber and other categories were found to have a higher accuracy of PA and UA compared to other land cover categories, as the accuracy of samples were minimized for these categories (Appendix A, Tables A1–A7).

The validation of the reference forest cover maps found that the Evergreen and Semi-Evergreen PA and US land cover categories had higher accuracy in both 2000 and 2005 (Table 5). In contrast, the Mixed woods and shrubs, Other forest and Non-forest categories yielded low UA and PA in both assessment years. Most of the confusion regarding Non-forest, Other forest, and Mixed woods and shrubs may have resulted from the lower accuracy or pixel difference of the refence maps. The distribution of Mixed woods and shrubs in most of the study area was considered as part of the Non-forest category, whereas Bamboo, Rubber plantation, and Flooded forest were considered as part of the other forest category. This could be the reason for the confusion of the Other forest categories with the Evergreen Semi-Evergreen and Deciduous categories. However, the overall accuracy of Evergreen and Semi-Evergreen improved in both validation maps (Appendix A, Tables A8 and A9).

There are possible errors in our study due to the resolution of remote sensing data, limited IPCC land cover category threshold values and the distribution of forest and non-forest land cover categories. One possible source of error is limited ground reference data. Different vegetation types at various growing stages show different phenological behavior [75] and their spectral values vary during phenological stages [75,76]. More field-based studies are needed to improve the accuracy of the PBTC method for the assessment of land use, land-use change, and forestry canopy disturbance, and carbon stock changes. If carbon emissions from all land use sectors are included in the assessment, the change detection approach would be appropriate [26,41].

Since we focused mainly on IPCC forest land cover category (i.e., the seven forest categories as shown in Table 7), more categories of land cover should be added to make our methods and results consistent with the land cover categories currently used by the Cambodian government for its forest resource assessment at the national level [59]. If such categories are added, the level of map accuracy might change [59], and so the forest carbon stock would also change. Therefore, future studies will need to focus on determining the threshold values for any new cover categories.

5. Conclusions

Using a combination of PBTC, GEE, and Landsat 5 and Landsat 8 OLI, we were able to classify seven forest cover categories in Siem Reap province, Cambodia over a 28-year period from 1990 to 2018. These categories are bamboo, plantation (Rubber), evergreen, semi-evergreen, deciduous, mixed woods and shrubs, and flooded forests. Evergreen forest suffered rapid loss (-1.8%) while rubber plantation increased by 109% annually. On average, 11,525 ha (1.3%) of forest cover were lost annually. This loss was responsible for 14,372,944 $MgCO_2$/year of the carbon emissions, of which 28% occurred in Svay Leu district alone. Using the retrospective approach, FREL for Siem Reap was estimated at 35,303,937 $MgCO_2$ $MgCO_2$/year during the Paris Agreement between 2020 and 2030. If REDD+ activities are implemented, 825,674.6 $MgCO_2$ of carbon emissions could be reduced annually over the same period. Depending on chosen carbon prices, result-based carbon revenues could be USD6 to 115 million annually.

The overall cumulative accuracy of this study was 92.1% and its cumulative Kappa was 0.9, which are sufficiently high to apply the PBTC method to detect forest land cover change. With these levels of overall accuracy, it is possible to conclude that PBTC and GEE fast cloud computing can be used to assess forest cover and carbon stock changes by category at any scale, quickly and without any costs. Such technologies become increasingly important for monitoring, measuring, reporting, and verifying the performance of the REDD+ activities in developing countries as required under the UNFCCC REDD+ scheme before they can claim for the result-based payments for their efforts in emission reductions or removals.

Our study demonstrated the capability of using the GEE cloud computing platform in combination with the PBTC method, and with the use of Landsat moderate resolution (30 m) remote sensing data, for estimating forest cover and carbon stock changes in a tropical developing country with limited retrospective data or resources to acquire direct or repeated measurements of forest carbon stocks in the field. Our methods, along with GEE and increasingly available satellite imagery, make it possible to perform the MRV tasks required under the REDD+ scheme of the UNFCCC and/or to detect land cover changes anywhere, at speed and scale.

Author Contributions: Conceptualization, M.V.; methodology, M.V.; GEE coding, M.V.; validation, M.V., N.S.; formal analysis, M.V.; investigation, M.V.; resources, N.S., B.S., S.A.; data curation, M.V.; writing—original draft preparation, M.V.; writing—review and editing, N.S., B.S., M.V.; visualization, M.V.; supervision, M.V., N.S., B.S., S.A.; project administration, M.V., N.S., B.S.; funding acquisition, N.S., B.S., M.V. All authors have read and agreed to the published version of the manuscript.

Conflicts of Interest: The authors declare no conflict of interest.

Appendix A

Table A1. Results of the accuracy assessment of the PBTC land cover map for 1990.

1990 LULC Categories	WA	OT	CR	Mix WS	DD	SEG	EG	BB	FF	User's Accuracy (%)
WA	6									100
OT		7	2						7	78
CR			59							100
Mix WS			1	45						98
DD				5	88	2				93
SEG					5	62	7			84
EG						6	59			91
BB						2		3		60
FF									60	100
Producer's accuracy (%)	100	100	95	90	95	89	87	100	100	Total Accuracy 92.84%

Kappa 0.91
Total reference points 419

Note: The accuracy assessment was validated using the Google Earth very high resolution imagery for the PBTC land cover category; Water (WA), Others (OT), Croplands (CR), Mixed Woods and Shrubs (Mix WS), Deciduous forest (DD), Semi-evergreen forest (SEG), Evergreen forest (EG), Bamboo (BB) and Flooded forest (FF), respectively. We used 419 5 × 5 km systematic reference points to validate the GEE PBTC threshold map in 1990. The highlighted gray cells indicate agreement of the accuracy matrix.

Table A2. Results of the accuracy assessment of the PBTC land cover map for 1995.

1995 LULC Category	WA	OT	CR	Mix WS	DD	SEG	EG	BB	FF	User's Accuracy (%)
WA	9									100
OT		4	1							80
CR		4	69	2						92
Mix WS			1	42	3					91
DD				1	98	2				97
SEG					8	58	1			87
EG						8	48			86
BB								2		100
FF									58	100
Producer's accuracy (%)	100	50	97	93	90	85	98	100	100	Total Accuracy 92.60%

Kappa 0.91
Total reference points 419

Table A3. Results of the accuracy assessment of the PBTC land cover map for 2000.

2000 LULC Category	WA	OT	CR	Mix WS	DD	SEG	EG	BB	FF	User's Accuracy (%)
WA	9									100
OT	2	7	2							64
CR		5	71	3						90
Mix WS			8	37						82
DD				4	99	1				95
SEG					1	57	2			95
EG						4	46		1	90
BB								2		100
FF									58	100
Producer's accuracy (%)	82	58	88	84	99	92	96	67	100	Total Accuracy 92.12%
				Kappa 0.91						
				Total reference points 419						

Table A4. Results of the accuracy assessment of the PBTC land cover map for 2005.

2005 LULC Category	WA	OT	CR	Mix WS	DD	SEG	EG	RB	BB	FF	User's Accuracy (%)
WA	10										100
OT	3	5	3								45
CR			85	2							98
Mix WS				45	3	1					92
DD				5	96	8					88
SEG				1		56					98
EG						3	32				91
RB											-
BB								1	3		75
FF										57	100
Producer's accuracy (%)	77	100	97	85	97	82	97	-	100	100	Total Accuracy 92.84%
				Kappa 0.91							
				Total reference points 419							

Table A5. Results of the accuracy assessment of the PBTC land cover map for 2010.

2010 LULC Category	WA	OT	CR	Mix WS	DD	SEG	EG	RB	BB	FF	User's Accuracy (%)
WA	5										100
OT	1	14	3								78
CR		1	86								99
Mix WS			4	37	3						84
DD			1	6	95	1					92
SEG					1	59	3	1			92
EG						5	31	1	1		82
RB											-
BB								1	2		67
FF			1							56	98
Producer's accuracy (%)	83	93	91	86	96	91	89	-	67	100	Total Accuracy 91.89%
				Kappa 0.90							
				Total reference points 419							

Table A6. Results of the accuracy assessment of the PBTC land cover map for 2015.

2015 LULC Category	WA	OT	CR	Mix WS	DD	SEG	EG	RB	BB	FF	User's Accuracy (%)
WA	6										100
OT	1	11	5								65
CR		2	150	8							94
Mix WS			3	23	2						82
DD			1	7	51	7					77
SEG						56		1	1		97
EG						2	22		1		88
RB								1			100
BB							1		3	1	60
FF			1							52	98
Producer's accuracy (%)	86	85	94	61	96	86	96	50	60	98	Total Accuracy 89.50%

Kappa 0.87
Total reference points 419

Table A7. Results of the accuracy assessment of the PBTC land cover map for 2018.

2018 LULC Category	WA	OT	CR	Mix WS	DD	SEG	EG	RB	BB	FF	User's Accuracy (%)
WA	10										100
OT		7	4								64
CR			153	6							96
Mix WS			3	31	2						86
DD			1	6	51	4					82
SEG				3		55		1	1		92
EG						2	19		1		86
RB								1	1		50
BB							1		3		75
FF			2							51	96
Producer's accuracy (%)	100	100	94	67	96	90	95	50	50	100	Total Accuracy 90.93%

Kappa 0.88
Total reference points 419

Table A8. Accuracy of the PBTC land cover map and referenced land cover map for 2000.

2000 Ref LULC Category	EG	SE	DD	Mix WS	OF	NF	User's Accuracy (%)
EG	48	4					92
SE	3	41	1	1			89
DD	1	2	54	6	2	1	82
Mix WS		1	5	36	2	1	80
OF	2	4	8	4	39	3	65
NF	2	3	6	8	8	123	82
Producer's accuracy (%)	86	75	73	65	76	96	Total Accuracy 81.38%

Kappa 0.77
Total reference points 419

Note: The accuracy assessment was validated for PBTC land cover classes using the referenced land cover data by assessing 419 5 × 5 km systematic reference points for land cover classes; Evergreen (EG), Semi-Evergreen (SG), Deciduous forest (DD), Mixed Woods and Shrubs (Mix WS), Other forest (OF), and Non-Forest (NF).

Table A9. Accuracy assessment of the PBTC land cover map and referenced land cover map for 2005.

2005 Ref LULC Category	EG	SE	DD	Mix WS	OF	NF	User's Accuracy (%)
EG	39	6	1	1		1	81
SE	2	37	1	1			90
DD	2	1	44	5	5		77
Mix WS	1	1	2	21			84
OF	2	4	4	1	65	2	83
NF	5	4	6	7	6	142	84
Producer's accuracy (%)	76	70	76	58	86	98	Total Accuracy 83.05%

Kappa 0.78
Total reference points 419

Table A10. Changes in forest cover by forest category in Siem Reap Province from 1990 to 2018.

Forest Category	Forest Category Area Cover (ha)						Forest Area Change (ha)			Rate (%)
	1990	1995	2000	2005	2010	2015	2018	1990–2018	Annual Change	
Evergreen Forest	188,332	186,923	178,249	157,350	142,451	127,240	91,254	97,078	3467	−1.8
Semi-Evergreen Forest	162,797	159,084	151,325	144,430	143,221	116,251	104,529	58,268	2081	−1.3
Deciduous Forest	240,205	232,976	233,940	228,943	226,331	181,153	173,010	67,194	2400	−1.0
Mixed Woods and Shrubs	130,876	127,360	121,764	136,065	146,432	67,562	68,782	62,095	2218	−1.7
Flooded Forest	141,083	140,331	130,415	112,502	107,614	79,966	79,662	61,420	2194	−1.6
Bamboo	6162	5600	5211	7768	8364	7276	8865	2703	97	+1.6
Rubber Plantation	0	0	0	388	2677	6219	20,658	20,658	738	+109.0
All forest Area (ha)	869,455	852,274	820,904	787,447	777,091	585,667	546,760	322,694	11,525	−1.3

Table A11. Carbon emissions, FREL, Project Emission, Reductions, and Carbon revenues in Siem Reap province from 1990 to 2030.

t	Year	EG (ha)	EG MgC	SEG (ha)	SEG MgC	DD (ha)	DD MgC	MiXWS (ha)	MiXWS MgC	FF (ha)	FF MgC	Total (ha)	Total (MgC)	Loss (MgC)	Emissions/FREL (MgCO$_2$)	PE (t) (MgCO$_2$)	Reduction (MgCO$_2$)	CR (USD Million)
-	1990	209,324	34,496,535	253,342	39,217,345	253,342	38,026,637	151,202	5,972,473	153,748	8,671,386	1,020,958	126,384,376	1,966,196	7,209,387			
1	1991	204,546	33,709,257	250,535	38,782,850	250,535	37,605,335	147,916	5,842,667	150,320	8,478,071	1,003,853	124,418,180	1,931,617	7,082,595			
2	1992	199,878	32,939,945	247,759	38,353,169	247,759	37,188,700	144,701	5,715,684	146,969	8,289,066	987,067	122,486,563	1,897,710	6,958,269			
3	1993	195,317	32,188,191	245,015	37,928,249	245,015	36,776,680	141,556	5,591,459	143,693	8,104,274	970,594	120,588,854	1,864,461	6,836,357			
4	1994	190,859	31,453,593	242,300	37,508,036	242,300	36,369,226	138,479	5,469,935	140,489	7,923,601	954,428	118,724,393	1,831,857	6,716,810			
5	1995	186,503	30,735,761	239,615	37,092,479	239,615	35,966,286	135,470	5,351,052	137,357	7,746,957	938,561	116,892,535	1,799,885	6,599,578			
6	1996	182,247	30,034,310	236,961	36,681,526	236,961	35,567,810	132,525	5,234,753	134,295	7,574,250	922,989	115,092,650	1,768,531	6,484,613			
7	1997	178,088	29,348,868	234,335	36,275,126	234,335	35,173,750	129,645	5,120,982	131,301	7,405,394	907,705	113,324,120	1,737,782	6,371,868			
8	1998	174,023	28,679,070	231,739	35,873,229	231,739	34,784,054	126,827	5,009,683	128,374	7,240,302	892,703	111,586,338	1,707,626	6,261,297			
9	1999	170,052	28,024,557	229,172	35,475,784	229,172	34,398,677	124,071	4,900,803	125,512	7,078,891	877,979	109,878,711	1,678,051	6,152,855			
10	2000	166,171	27,384,981	226,633	35,082,742	226,633	34,017,569	121,374	4,794,289	122,714	6,921,078	863,525	108,200,660	1,649,045	6,046,498			
11	2001	162,379	26,760,002	224,122	34,694,056	224,122	33,640,683	118,736	4,690,091	119,978	6,766,783	849,337	106,551,615	1,620,595	5,942,183			
12	2002	158,673	26,149,287	221,639	34,309,675	221,639	33,267,973	116,156	4,588,157	117,304	6,615,928	835,410	104,931,020	1,592,691	5,839,868			
13	2003	155,052	25,552,509	219,183	33,929,553	219,183	32,899,392	113,631	4,488,438	114,689	6,468,436	821,738	103,338,328	1,565,321	5,739,511			
14	2004	151,513	24,969,350	216,755	33,553,643	216,755	32,534,895	111,162	4,390,887	112,132	6,324,232	808,316	101,773,007	1,538,474	5,641,072			
15	2005	148,055	24,399,501	214,353	33,181,897	214,353	32,174,436	108,746	4,295,456	109,632	6,183,243	795,140	100,234,533	1,512,140	5,544,513			
16	2006	144,676	23,842,656	211,978	32,814,270	211,978	31,817,971	106,382	4,202,099	107,188	6,045,397	782,203	98,722,393	1,486,307	5,449,793			
17	2007	141,375	23,298,520	209,630	32,450,716	209,630	31,465,455	104,070	4,110,771	104,798	5,910,625	769,503	97,236,086	1,460,966	5,356,875			
18	2008	138,148	22,766,802	207,307	32,091,190	207,307	31,116,845	101,808	4,021,428	102,462	5,778,856	757,033	95,775,120	1,436,106	5,265,723			
19	2009	134,995	22,247,219	205,011	31,735,647	205,011	30,772,097	99,596	3,934,027	100,178	5,650,026	744,790	94,339,014	1,411,718	5,176,299			
20	2010	131,914	21,739,494	202,739	31,384,043	202,739	30,431,168	97,431	3,848,525	97,944	5,524,067	732,768	92,927,296	1,387,792	5,088,570			
21	2011	128,904	21,243,356	200,493	31,036,334	200,493	30,094,017	95,313	3,764,881	95,761	5,400,916	720,964	91,539,504	1,364,318	5,002,499			
22	2012	125,962	20,758,541	198,272	30,692,478	198,272	29,760,601	93,242	3,683,056	93,626	5,280,511	709,374	90,175,186	1,341,287	4,918,053			
23	2013	123,087	20,284,790	196,075	30,352,432	196,075	29,430,879	91,215	3,603,009	91,539	5,162,790	697,992	88,833,899	1,318,691	4,835,199			
24	2014	120,278	19,821,851	193,903	30,016,153	193,903	29,104,810	89,233	3,524,701	89,498	5,047,694	686,815	87,515,209	1,296,519	4,753,905			
25	2015	117,533	19,369,478	191,755	29,683,599	191,755	28,782,353	87,294	3,448,096	87,503	4,935,163	675,839	86,218,689	1,274,765	4,674,138			
26	2016	114,851	18,927,428	189,630	29,354,730	189,630	28,463,469	85,396	3,373,155	85,552	4,825,141	665,059	84,943,924	1,253,418	4,595,867			
27	2017	112,230	18,495,467	187,529	29,029,505	187,529	28,148,118	83,540	3,299,843	83,645	4,717,572	654,473	83,690,506	1,232,472	4,519,063			
28	2018	109,668	18,073,364	185,451	28,707,883	185,451	27,836,261	81,725	3,228,125	81,780	4,612,401	644,076	82,458,034	1,211,917	4,443,694			
29	2019	107,166	17,660,894	183,397	28,389,824	183,397	27,527,859	79,948	3,157,965	79,957	4,509,575	633,865	81,246,118	1,191,745	4,369,733			
30	2020	104,720	17,257,838	181,365	28,075,289	181,365	27,222,874	78,211	3,089,330	78,174	4,409,041	623,835	80,054,372	1,171,950	4,297,151	4,297,151	-	-
31	2021	102,330	16,863,980	179,356	27,764,239	179,356	26,921,268	76,511	3,022,187	76,432	4,310,748	613,984	78,882,422	1,152,523	4,225,919	4,177,059	48,860	342,021
32	2022	99,995	16,479,111	177,368	27,456,635	177,368	26,623,003	74,848	2,956,503	74,728	4,214,647	604,307	77,729,899	1,133,457	4,156,010	3,999,842	156,168	1,093,178
33	2023	97,713	16,103,026	175,403	27,152,439	175,403	26,328,043	73,221	2,892,247	73,062	4,120,688	594,803	76,596,442	1,114,745	4,087,398	3,260,374	827,024	5,789,166
34	2024	95,483	15,735,523	173,460	26,851,613	173,460	26,036,351	71,630	2,829,387	71,433	4,028,823	585,466	75,481,697	1,096,379	4,020,056	3,078,839	941,218	6,588,525
35	2025	93,303	15,376,407	171,538	26,554,120	171,538	25,747,890	70,073	2,767,894	69,841	3,939,007	576,294	74,385,318	1,078,353	3,953,960	2,891,070	1,062,890	7,440,227
36	2026	91,174	15,025,488	169,638	26,259,923	169,638	25,462,625	68,550	2,707,737	68,284	3,851,193	567,283	73,306,965	1,060,659	3,889,083	2,832,392	1,056,691	7,396,837
37	2027	89,093	14,682,576	167,758	25,968,985	167,758	25,180,521	67,060	2,648,887	66,761	3,765,336	558,432	72,246,306	1,043,291	3,825,401	2,774,955	1,050,445	7,353,118
38	2028	87,060	14,347,491	165,900	25,681,271	165,900	24,901,543	65,603	2,591,316	65,273	3,681,394	549,735	71,203,015	1,026,243	3,762,890	2,718,733	1,044,157	7,309,098
39	2029	85,073	14,020,053	164,062	25,396,745	164,062	24,625,655	64,177	2,534,997	63,818	3,599,323	541,191	70,176,772	1,009,507	3,701,527	2,663,698	1,037,829	7,264,800
40	2030	83,132	13,700,088	162,244	25,115,370	162,244	24,352,823	62,782	2,479,901	62,395	3,519,081	532,797	69,167,265	993,079	3,641,289	2,609,824	1,031,464	7,220,249
								Total: Project emissions, Reductions and Carbon credits over a 10-year project from 2020 to 2030									35,303,937	8,256,746	57,797,219

Note: Forest reference emission levels (FREL) are equivalent to carbon emissions starting from 2020 through 2030. Emission reductions and carbon revenues were estimated only for the 2020–2030 period.

References

1. Hughes, A.C. Understanding the drivers of Southeast Asian biodiversity loss. *Ecosphere* **2017**, *8*, e01624. [CrossRef]
2. Vibol, S.; Towprayoon, S. Estimation of methane and nitrous oxide emissions from rice field with rice straw management in Cambodia. *Environ. Monit. Assess.* **2010**, *161*, 301–313. [CrossRef]
3. Hansen, M.C.; Potapov, P.V.; Moore, R.; Hancher, M.; Turubanova, S.A.; Tyukavina, A.; Thau, D.; Stehman, S.V.; Goetz, S.J.; Loveland, T.R.; et al. High-resolution global maps of 21st-century forest cover change. *Science* **2013**, *342*, 850–853. [CrossRef]
4. Asner, G.P.; Rudel, T.K.; Aide, T.M.; Defries, R.; Emerson, R. A contemporary assessment of change in humid tropical forests. *Conserv. Biol.* **2009**, *23*, 1386–1395. [CrossRef] [PubMed]
5. Blaser, J.; Johnson, S.; Poore, D.; Sarre, A. *Status of Tropical Forest Management 2011 Status of Tropical Forest Management*; International Tropical Timber Organisation: Jokohama, Japan, 2011.
6. *FAO Global Forest Resources Assessment 2020—Key Findings*; FAO: Rome, Italy, 2020; p. 16.
7. Le Quéré, C.; Moriarty, R.; Andrew, R.M.; Canadell, J.G.; Sitch, S.; Korsbakken, J.I.; Friedlingstein, P.; Peters, G.P.; Andres, R.J.; Boden, T.A.; et al. Global Carbon Budget 2015. *Earth Syst. Sci. Data* **2015**, *7*, 349–396. [CrossRef]
8. Alexander, S.; Nelson, C.R.; Aronson, J.; Lamb, D.; Cliquet, A.; Erwin, K.L.; Finlayson, C.M.; de Groot, R.S.; Harris, J.A.; Higgs, E.S.; et al. Opportunities and Challenges for Ecological Restoration within REDD+. *Restor. Ecol.* **2011**, *19*, 683–689. [CrossRef]
9. Sasaki, N.; Asner, G.P.; Pan, Y.; Knorr, W.; Durst, P.B.; Ma, H.O.; Abe, I.; Lowe, A.J.; Koh, L.P.; Putz, F.E. Sustainable Management of Tropical Forests Can Reduce Carbon Emissions and Stabilize Timber Production. *Front. Environ. Sci.* **2016**, *4*, 50. [CrossRef]
10. Sasaki, N.; Chheng, K.; Mizoue, N.; Abe, I.; Lowe, A.J. Forest reference emission level and carbon sequestration in Cambodia. *Glob. Ecol. Conserv.* **2016**, *7*, 82–96. [CrossRef]
11. Sasaki, N.; Abe, I.; Khun, V.; Chan, S.; Ninomiya, H.; Chheng, K. Reducing Carbon Emissions through Improved Forest Management in Cambodia. *Low Carbon Econ.* **2013**, *4*, 55–67. [CrossRef]
12. Chave, J.; Andalo, C.; Brown, S.; Cairns, M.A.; Chambers, J.Q.; Eamus, D.; Fölster, H.; Fromard, F.; Higuchi, N.; Kira, T.; et al. Tree allometry and improved estimation of carbon stocks and balance in tropical forests. *Oecologia* **2005**, *145*, 87–99. [CrossRef]
13. Kenzo, T.; Ichie, T.; Hattori, D.; Kendawang, J.J.; Sakurai, K.; Ninomiya, I. Changes in above- and belowground biomass in early successional tropical secondary forests after shifting cultivation in Sarawak, Malaysia. *For. Ecol. Manag.* **2010**, *260*, 875–882. [CrossRef]
14. Gibbs, H.K.; Brown, S.; Niles, J.O.; Foley, J.A. Monitoring and estimating tropical forest carbon stocks: Making REDD a reality. *Environ. Res. Lett.* **2007**, *2*, 045023. [CrossRef]
15. Aronson, J.; Vallejo, R. *Monitoring and Evaluating Forest Restoration Success*; Springer: New York, NY, USA, 2014.
16. Chheng, K.; Sasaki, N.; Mizoue, N.; Khorn, S.; Kao, D.; Lowe, A. Assessment of carbon stocks of semi-evergreen forests in Cambodia. *Glob. Ecol. Conserv.* **2016**, *5*, 34–47. [CrossRef]
17. Hemingway, H.J.; Kimsey, M.M. Defining and Estimating Forest Productivity Using Multi-Point Measures and a Nonparametric Approach. *For. Sci.* **2020**. [CrossRef]
18. Clark, N.A.; Wynne, R.H.; Schmoldt, D.L. A review of past research on dendrometers. *For. Sci.* **2000**, *46*, 570–576.
19. Coppin, P.; Jonckheere, I.; Nackaerts, K.; Muys, B.; Lambin, E. Review ArticleDigital change detection methods in ecosystem monitoring: A review. *Int. J. Remote Sens.* **2004**, *25*, 1565–1596. [CrossRef]
20. Helman, D. Land surface phenology: What do we really 'see' from space? *Sci. Total Environ.* **2018**, *618*, 665–673. [CrossRef]
21. Kou, W.; Xiao, X.; Dong, J.; Gan, S.; Zhai, D.; Zhang, G.; Qin, Y.; Li, L. Mapping deciduous rubber plantation areas and stand ages with PALSAR and landsat images. *Remote Sens.* **2015**, *7*, 1048–1073. [CrossRef]
22. Brooks, E.B.; Thomas, V.A.; Wynne, R.H.; Coulston, J.W. Fitting the multitemporal curve: A fourier series approach to the missing data problem in remote sensing analysis. *IEEE Trans. Geosci. Remote Sens.* **2012**, *50*, 3340–3353. [CrossRef]

23. Kiptala, J.K.; Mohamed, Y.; Mul, M.L.; Cheema, M.J.M.; Van Der Zaag, P. Land use and land cover classification using phenological variability from MODIS vegetation in the Upper Pangani River Basin, Eastern Africa. *Phys. Chem. Earth* **2013**, *66*, 112–122. [CrossRef]

24. Venkatappa, M.; Sasaki, N.; Shrestha, R.P.; Tripathi, N.K.; Ma, H.O. Determination of vegetation thresholds for assessing land use and land use changes in Cambodia using the Google Earth Engine cloud-computing platform. *Remote Sens.* **2019**, *11*, 1514. [CrossRef]

25. Adole, T.; Dash, J.; Atkinson, P.M. Characterising the land surface phenology of Africa using 500 m MODIS EVI. *Appl. Geogr.* **2018**, *90*, 187–199. [CrossRef]

26. Langner, A.; Miettinen, J.; Kukkonen, M.; Vancutsem, C.; Simonetti, D.; Vieilledent, G.; Verhegghen, A.; Gallego, J.; Stibig, H.J. Towards operational monitoring of forest canopy disturbance in evergreen rain forests: A test case in continental Southeast Asia. *Remote Sens.* **2018**, *10*, 544. [CrossRef]

27. Schwieder, M.; Leitão, P.J.; Pinto, J.R.R.; Teixeira, A.M.C.; Pedroni, F.; Sanchez, M.; Bustamante, M.M.; Hostert, P. Landsat phenological metrics and their relation to aboveground carbon in the Brazilian Savanna. *Carbon Balance Manag.* **2018**, *13*, 7. [CrossRef] [PubMed]

28. Simonetti, D.; Simonetti, E.; Szantoi, Z.; Lupi, A.; Eva, H.D. First Results from the Phenology-Based Synthesis Classifier Using Landsat 8 Imagery. *IEEE Geosci. Remote Sens. Lett.* **2015**, *12*, 1496–1500. [CrossRef]

29. Tsai, Y.H.; Stow, D.; Chen, H.L.; Lewison, R.; An, L.; Shi, L. Mapping vegetation and land use types in Fanjingshan National Nature Reserve using google earth engine. *Remote Sens.* **2018**, *10*, 927. [CrossRef]

30. Xiong, J.; Thenkabail, P.S.; Tilton, J.C.; Gumma, M.K.; Teluguntla, P.; Oliphant, A.; Congalton, R.G.; Yadav, K.; Gorelick, N. Nominal 30-m cropland extent map of continental Africa by integrating pixel-based and object-based algorithms using Sentinel-2 and Landsat-8 data on google earth engine. *Remote Sens.* **2017**, *9*, 1065. [CrossRef]

31. Li, M.; Zang, S.; Zhang, B.; Li, S.; Wu, C. A Review of Remote Sensing Image Classification Techniques: The Role of Spatio-contextual Information. *Eur. J. Remote Sens.* **2014**, *47*, 389–411. [CrossRef]

32. Xie, Y.; Sha, Z.; Yu, M. Remote sensing imagery in vegetation mapping: A review. *J. Plant Ecol.* **2008**, *1*, 9–23. [CrossRef]

33. Chen, G.; Hay, G.J.; Carvalho, L.M.T.; Wulder, M.A. Object-based change detection. *Int. J. Remote Sens.* **2012**, *33*, 4434–4457. [CrossRef]

34. Lu, D.; Weng, Q. A survey of image classification methods and techniques for improving classification performance. *Int. J. Remote Sens.* **2007**, *28*, 823–870. [CrossRef]

35. Bey, A.; Díaz, A.S.P.; Maniatis, D.; Marchi, G.; Mollicone, D.; Ricci, S.; Bastin, J.-F.F.; Moore, R.; Federici, S.; Rezende, M.; et al. Collect earth: Land use and land cover assessment through augmented visual interpretation. *Remote Sens.* **2016**, *8*, 807. [CrossRef]

36. Romijn, E.; Lantican, C.B.; Herold, M.; Lindquist, E.; Ochieng, R.; Wijaya, A.; Murdiyarso, D.; Verchot, L. Assessing change in national forest monitoring capacities of 99 tropical countries. *For. Ecol. Manag.* **2015**, *352*, 109–123. [CrossRef]

37. Gorelick, N.; Hancher, M.; Dixon, M.; Ilyushchenko, S.; Thau, D.; Moore, R. Google Earth Engine: Planetary-scale geospatial analysis for everyone. *Remote Sens. Environ.* **2017**, *202*, 18–27. [CrossRef]

38. Zhang, M.; Lin, H. Object-based rice mapping using time-series and phenological data. *Adv. Sp. Res.* **2018**, *63*, 190–202. [CrossRef]

39. Fan, H.; Fu, X.; Zhang, Z.; Wu, Q.; Fan, H.; Fu, X.; Zhang, Z.; Wu, Q. Phenology-Based Vegetation Index Differencing for Mapping of Rubber Plantations Using Landsat OLI Data. *Remote Sens.* **2015**, *7*, 6041–6058. [CrossRef]

40. Zhou, Y.; Xiao, X.; Qin, Y.; Dong, J.; Zhang, G.; Kou, W.; Jin, C.; Wang, J.; Li, X. Mapping paddy rice planting area in rice-wetland coexistent areas through analysis of Landsat 8 OLI and MODIS images. *Int. J. Appl. Earth Obs. Geoinf.* **2016**, *46*, 1–12. [CrossRef]

41. Mitchell, A.L.; Rosenqvist, A.; Mora, B. Current remote sensing approaches to monitoring forest degradation in support of countries measurement, reporting and verification (MRV) systems for REDD+. *Carbon Balance Manag.* **2017**, *12*, 9. [CrossRef]

42. Gaughan, A.E.; Binford, M.W.; Southworth, J. Tourism, forest conversion, and land transformations in the Angkor basin, Cambodia. *Appl. Geogr.* **2009**, *29*, 212–223. [CrossRef]

43. MoA Climate Change Priorities Action Plan for Agriculture, Forestry and Fisheries Sector 2016–2020. Available online: http://www.twgaw.org/wp-content/uploads/2016/08/MAFF-CCPAP-2016-2020_final_CLEAN.pdf (accessed on 19 November 2018).

44. National Institute of Statistics General Population Census of Cambodia 2019. Available online: https://www.nis.gov.kh/index.php/en/15-gpc/79-press-release-of-the-2019-cambodia-general-population-census (accessed on 26 August 2020).

45. TC Cambodia Tourism Statistics–Tourist Information Center | Tourism Cambodia. Available online: https://www.tourismcambodia.com/tourist-information/tourist-statistic.htm (accessed on 29 July 2020).

46. Chan, S.; Sasaki, N. Assessment of Drivers of Deforestation and Forest Degradation in Phnom Tbeng Forest Based on Socio-Economic Surveys. *J. Environ. Prot.* **2014**, *5*, 1641–1653. [CrossRef]

47. NIS. National Institute of Statistics. Available online: http://www.nis.gov.kh/index.php/en/ (accessed on 19 August 2020).

48. ODC. Open Development Cambodia. Available online: https://opendevelopmentcambodia.net/map-explorer (accessed on 17 August 2020).

49. Chander, G.; Markham, B.L.; Helder, D.L. Summary of current radiometric calibration coefficients for Landsat MSS, TM, ETM+, and EO-1 ALI sensors. *Remote Sens. Environ.* **2009**, *113*, 893–903. [CrossRef]

50. Sidhu, N.; Pebesma, E.; Câmara, G. Using Google Earth Engine to detect land cover change: Singapore as a use case. *Eur. J. Remote Sens.* **2018**, *51*, 486–500. [CrossRef]

51. Kou, W.; Liang, C.; Wei, L.; Hernandez, A.; Yang, X. Phenology-Based Method for Mapping Tropical Evergreen Forests by Integrating of MODIS and Landsat Imagery. *Forests* **2017**, *8*, 34. [CrossRef]

52. Jiang, Z.; Huete, A.R.; Didan, K.; Miura, T.; Ramirez-Reyes, C.; Brauman, K.A.; Chaplin-Kramer, R.; Galford, G.L.; Adamo, S.B.; Anderson, C.B.C.; et al. Reimagining the potential of Earth observations for ecosystem service assessments. *Remote Sens. Environ.* **2019**, *112*, 3833–3845. [CrossRef]

53. IPCC. Task Force on National Greenhouse Gas Inventories. Available online: https://www.ipcc-nggip.iges.or.jp/public/2006gl/vol4.html (accessed on 10 June 2020).

54. Potere, D. Horizontal positional accuracy of google earth's high-resolution imagery archive. *Sensors* **2008**, *8*, 7973–7981. [CrossRef]

55. Tilahun, A. Accuracy Assessment of Land Use Land Cover Classification using Google Earth. *Am. J. Environ. Prot.* **2015**, *4*, 193. [CrossRef]

56. Ragheb, A.E.; Ragab, A.F. Enhancement of Google Earth Positional Accuracy. *Int. J. Eng. Res. Technol.* **2015**, *4*, 627–630.

57. Mohammed, N.Z.; Ghazi, A.; Mustafa, H.E. Positional accuracy testing of Google Earth. *Int. J. Multidiscip. Sci. Eng.* **2013**, *4*, 6–9.

58. Olofsson, P.; Foody, G.M.; Herold, M.; Stehman, S.V.; Woodcock, C.E.; Wulder, M.A. Good practices for estimating area and assessing accuracy of land change. *Remote Sens. Environ.* **2014**, *148*, 42–57. [CrossRef]

59. FREL. Initial Forest Reference Level for Cambodia under the UNFCCC Framework. Available online: https://redd.unfccc.int/files/cambodia_frl_rcvd17112016.pdf (accessed on 17 November 2018).

60. Denniss, A.T.M.; Lillesand, R.W.; Kiefer, R.W. *Remote Sensing and Image Interpretation*, 3rd ed.; John Wiley & Sons: New York, NY, USA, 1994; Volume xvi, p. 750, ISBN 0471577839. [CrossRef]

61. UN-REDD Programme. *Technical Considerations for Forest Reference Emission Level and/or Forest Reference Level construction for REDD+ under the UNFCCC*; United Nations REDD Programme: Geneva, Switzerland, 2015; ISBN 9789251088418.

62. Ty, S.; Sasaki, N.; Ahmad, A.H.; Ahmad, Z.A. REDD Development in Cambodia-Potential Carbon Emission Reductions in a REDD Project. *Formath* **2011**, *10*, 1–23. [CrossRef]

63. World Bank; Ecofys. *State and Trends of Carbon Pricing 2018 by Word Bank Group*; World Bank: Washington, DC, USA, 2018.

64. Anderson, J.R.; Hardy, E.E.; Roach, J.T.; Witmer, R.E. *Land Use and Land Cover Classification System for use With Remote Sensor Data*; US Government Printing Office: Washington, DC, USA, 1976.

65. John, R.; Jensen, B.Y.U. *Introductory Digital Image Processing: A Remote Sensing Perspective*, 4th ed.; Prentice Hall Press: New York, NJ, USA, 2015.

66. MoE Cambodia Forest Cover 2016. Available online: https://redd.unfccc.int/uploads/54_3_cambodia_forest_cover_resource__2016_english.pdf (accessed on 10 June 2020).

67. Chim, K.; Tunnicliffe, J.; Shamseldin, A.; Ota, T. Land Use Change Detection and Prediction in Upper Siem Reap River, Cambodia. *Hydrology* **2019**, *6*, 64. [CrossRef]

68. Davis, K.F.; Yu, K.; Rulli, M.C.; Pichdara, L.; D'Odorico, P. Accelerated deforestation driven by large-scale land acquisitions in Cambodia. *Nat. Geosci.* **2015**, *8*, 772–775. [CrossRef]

69. IUCN. Flooded forest fires: A major threat to the Tonle Sap. Available online: https://www.iucn.org/news/cambodia/201607/flooded-forest-fires-major-threat-tonle-sap (accessed on 28 August 2020).

70. Sabogal, C.; Besacier, C.; McGuire, D. Forest and landscape restoration: Concepts, approaches and challenges for implementation. *Unasylva* **2015**, *66*, 3–10.

71. Perrin, A. Climate-smart agriculture. *Spore* **2015**, *2015*, 18–21.

72. Tubiello, F.N.; Salvatore, M.; Cóndor Golec, R.D.; Ferrara, A.; Rossi, S.; Biancalani, R.; Federici, S.; Jacobs, H.; Flammini, A. *Agriculture, Forestry and Other Land Use Emissions by Sources and Removals by Sinks*; FAO: Rome, Italy, 2014; Volume 2.

73. Tubiello, F.N.; Salvatore, M.; Rossi, S.; Ferrara, A.; Fitton, N.; Smith, P. The FAOSTAT database of greenhouse gas emissions from agriculture. *Environ. Res. Lett.* **2013**, *8*, 15009. [CrossRef]

74. STR. Sustainable travel and the impact of climate change on tourist perceptions | STR. Available online: https://str.com/data-insights-blog/sustainable-travel (accessed on 29 August 2020).

75. Nath, A.J.; Das, G.; Das, A.K. Vegetative phenology of three bamboo species in subtropical humid climate of Assam. *Trop. Ecol.* **2008**, *49*, 85–89.

76. Fava, F.; Colombo, R. Remote sensing-based assessment of the 2005–2011 bamboo reproductive event in the arakan mountain range and its relation with wildfires. *Remote Sens.* **2017**, *9*, 85. [CrossRef]